Algorithmic Quantum Heat Engines

by

Ş. Emre Köse

A Dissertation Submitted to the
Graduate School of Sciences and Engineering
in Partial Fulfillment of the Requirements for
the Degree of

Master of Science

in

Physics

KOÇ
UNIVERSITY

August 22, 2019

Algorithmic Quantum Heat Engines

Koç University

Graduate School of Sciences and Engineering

This is to certify that I have examined this copy of a master's thesis by

Ş. Emre Köse

and have found that it is complete and satisfactory in all respects,
and that any and all revisions required by the final
examining committee have been made.

Committee Members:

_____

Prof. Özgür E. Müstecaplıoğlu

_____

Prof. Tekin Dereli

_____

Asst. Prof. Barış Çakmak

Date: _____

To my mother...

ABSTRACT

In this thesis, we suggest alternative quantum Otto engines, using heat bath algorithmic cooling with partner pairing algorithm instead of isochoric cooling and quantum SWAP operations instead of quantum adiabatic processes. Liquid state nuclear magnetic resonance systems in a single entropy sink are threated as working fluids. The extractable work and thermal efficiency are analyzed in detail for four-stroke and two-stroke type of alternative quantum Otto engines. The role of the heat bath algorithmic cooling in these cycles is to use a single entropy sink instead of two so that a single incoherent energy resource can be harvested and processed using algorithmic quantum heat engine. Our results indicate a path to programmable quantum heat engines as analogues of quantum computers beyond traditional heat engine cycles. We find that for our NMR system example, implementation of quantum algorithmic heat engine stages yields more power due to increased cycle speeds [1].

ÖZETÇE

Bu tez çalışmasında kuantum Otto döngüsüne alternatif bir yöntem öneriyoruz. Izokorik soğutma yerine eş eşleştirmeli algoritmalı ısı banyosu algoritma soğutması ve kuantum adyabatik süreç yerine de kuantum değiştirme operatörlerini kullandık. Aracı akışkan olarak ise tek entropili ısı emicideki sıvı haldeki nükleer manyetik rezonans sistemlerini kullandık. Elde edilebilen iş ve termal verimliği 4 zamanlı ve 2 zamanlı kuantum Otto döngüleri için inceledik. Isı banyosunun algoritmik soğutmadaki işlevi motor çevrimlerinde çift yerine tek entropili ısı emici kullanarak eşevresiz enerji kaynaklarının da hem depolanabilmesi hem de işlenebilmesidir. Sonuçlarımız programlanabilir kuantum ısı makinelerinin geleneksel ısı makineleri çevrimlerindense kuantum bilgisayarlara benzer şekilde olduğuna işaret ediyor. NMR sistemi örneğimizde kuantum algoritmik ısı motorunun uygulanması artan döngü hızı sebebiyle daha fazla güç elde ettik.

ACKNOWLEDGMENTS

I would like to express my deep gratitude to my advisor Prof. Özgür E. Müstecaplıoğlu for giving me the opportunity to be a member of the Quest team. He has always inspired and motivated me through his lectures, his collaborations and the people he introduced me with. Above all, I am grateful for his patient guidance, enthusiastic encouragement and useful critiques at every stage of my master's degree. In the end, I will always feel indebted to him for his extraordinary kindness and generosity.

Besides my advisor, I would like to thank the rest of my thesis committee: Prof. Tekin Dereli and Asst Prof. Barış Çakmak for their insightful comments and encouragement, but also for the hard question which widen my research perspective. I am immensely grateful to Selçuk Çakmak for the inspiration to begin this research and the encouragement to carry on during the hard times.

I thank every member of our team, especially Cahit Kargı and Ricardo R. Ancheyta for our fruitful discussions, being very good friends, and colleagues. I am grateful to Elif Yunt, Aslı Tuncer, Onur Pusuluk, M. Tahir Naseem, Mohsen Izadyari, Serhat Kadıoğlu and Mojde Fadaie for being excellent teammates, always helping me in many stages of my thesis, and for their kind supporting personalities. Thanks to my flatmates Beakal and Cemil and many friends at Koç University for their friendships.

Beyond the words, I thank the hospitality of Iannis Kominis for giving me the opportunity to work on their experiment and supporting me during my visit. I am grateful to Kostas Mouloudakis for our interesting and useful discussions. In addition, I thank Antonis Margaritakis and Georgia Anyfantaki for their kind friendships.

Last but not least, many thanks to the love of my life, Gizem Özcan for supporting me spiritually throughout this study.

TABLE OF CONTENTS

LIST OF TABLES

LIST OF FIGURES

Chapter 1

INTRODUCTION

With the advances of miniaturized information and energy devices, the question of whether using a quantum system to harvest a classical resource can have an advantage over a classical harvester has gained much attention in recent years [5, 5–10, 10–28]. The argument is more or less settled in the case of quantum information devices, and the main challenge remained is their efficient implementation. In typical quantum information devices, both the inputs and the algorithmic steps of operation are of completely quantum nature. In contrast, quantum energy devices process incoherent inputs and they operate with thermodynamical processes being quantum analogues of their classical counterparts. The quantum superiority in such a thermal device reveals itself when the resource has some quantum character, for example, squeezing [29, 30], or when the harvester has profound quantum nature, for example, quantum correlations [31, 32]. Studies of both cases are limited to machine processes analogues of classical thermodynamical ones. Here we ask how can we use genuine quantum steps in the machine operation and if we can do so what are the quantum advantages we can get.

As a specific system to explore completely quantum steps in thermal quantum device operation we examine an NMR system. Very recently NMR quantum heat engines become experimentally available [33, 34]. Power outputs of these machines are not optimized. One can use non-classical resources, though such a resource would not be natural and may require some generation cost reducing overall operational efficiency. Alternatively one can use dynamical shortcuts to speeding up adiabatic transformations [35] but this would increase experimental complexity, and moreover

in NMR thermalization is more seriously slow step reducing the power output of the NMR machines.

Here, we propose to replace adiabatic steps by SWAP operations while the cooling step by an algorithmic cooling [2–4, 36–46]. By this way, NMR thermal device operation would closely resemble an NMR quantum computer [47–50] albeit processing a completely noisy input. We remark that there will be only the classical energy source as the input to the machine, while the second heat bath required by the second law of thermodynamics for work production would be an effective one, engineered by a spin ensemble, typical in the algorithmic cooling scheme. In addition to engine cycles, NMR systems were also proposed for studies of single-shot thermodynamics [51].

Our scheme allows us to provide at least one answer, in the context of NMR heat engines, to the question of how to implement genuine quantum steps in quantum machine operation to harvest a classical energy source. In addition, our calculations suggest that compared to the NMR engine with standard thermodynamical steps quantum algorithmic NMR engine produce more power. The advantage comes from replacing the long-time isochoric cooling process with the more efficient and fast algorithmic cooling stage. We provide systematic investigation by first examining the case of standard Otto cycle as a benchmark then introduce the algorithmic cooling stage instead of isochoric cooling one, and finally introduce the SWAP operation stages instead of the adiabatic transformations. Our results here can be seen as an example for a broader fundamental perspective that quantum computation processes can be used for efficient harvesting and processing both the coherent information and the incoherent energy resources. From a practical point of view our approach suggests that quantum heat engines can be programmed as analogue quantum computers beyond traditional engine cycles.

In this thesis, quantum thermodynamic processes and quantum heat engines, which are the quantum mechanical counterparts of classical thermodynamic processes and heat engines, are discussed. The algorithmic quantum Otto engines were simulated with the help of heat bath algorithmic cooling technique by considering a

applicable molecule on NMR, a physical system, and the necessary protocols were explained. In addition, using the quantum Otto cycle, work and efficiency calculations were made on NMR spin systems and the effects of the parameters in the model on the cycle were explained.

The organization of the thesis is as follows. We introduced the background for algorithmic heat engines in Chap. 2. In Chap. 3, we have explained the four stroke algorithmic quantum heat engines. Efficiency, work, and power output of the engine is discussed. The two-stroke-type algorithmic engine results are given in Chap. 4. We conclude in Chap. 5. The details of the cost of cooling using HBAC with a partner pairing algorithm (PPA) are given in Appendix A.

Chapter 2

BACKGROUND

In this chapter, we will briefly give the theoretical information about quantum mechanical foundations, open and closed quantum system dynamics, quantum thermodynamics, quantum information processing and heat bath algorithmic cooling method.

2.1 Quantum Mechanics; Closed Quantum Systems

In non-relativistic quantum mechanics, the evolution of the isolated quantum system can be described by the Schrödinger, the Heisenberg, and the interaction (Dirac) pictures [52–58]. In the Schrödinger picture time evolution operator affects the state vectors, while in the Heisenberg picture, instead of state vectors, observables evolve in time. For a given Hamiltonian $\hat{H}$, energy eigen vectors $|\psi_i\rangle$ form a complete basis set in the Hilbert space [59]. We can obtain eigen vectors from eigenvalue equation as

$$\hat{H}|\psi_i\rangle = E_i|\psi_i\rangle \tag{2.1}$$

A pure state $|\Psi\rangle$ can be defined as superposition state from the energy eigenstates as

$$|\Psi\rangle = \sum_i c_i|\psi_i\rangle \tag{2.2}$$

with normalization condition $\langle\Psi|\Psi\rangle = I$, where c_i are complex numbers. The pure states evolves in time due to the Schrödinger equation as

$$i\hbar\frac{\partial}{\partial t}|\Psi(t)\rangle = H(t)|\Psi(t)\rangle \tag{2.3}$$

where $\hbar$ is the Planck's constant and we can set it to the 1 for simplicity. The solution of the equation easly can be written as $|\Psi(t)\rangle = U(t,t_0)|\Psi(t_0)\rangle$ where $U(t,t_0)$ is the

unitary time evolution operator, which transform the initial state $|\Psi(t_0)\rangle$ at t_0 to final state $|\Psi(t)\rangle$ at time t. Initially the unitary operator is identity $U(t_0, t_0) = I$. If the Hamiltonian is time independent then the unitary evolution becomes

$$U(t, t_0) = e^{-iH(t-t_0)} \tag{2.4}$$

For the time dependent Hamiltonian it can be represented as a time ordering exponential

$$U(t, t_0) = T_{\leftarrow} e^{\int_{t_0}^{t} dt' H(t')} \tag{2.5}$$

where T is the time ordering operator. Before continue further, I will introduce density matrix formalism. It is first described by J. von Neumann in 1927. Let us consider an ensemble of an quantum system. If it is pure ensemble, every member of the ensemble characterized by the same state. On the other hand, for a mixed ensemble, parts of the population with some weights w_i are in the same states. One can easily see that the mixed ensemble can be considered as a mixture of pure ensembles. If we have an observable $\mathcal{O}$, using the statistical weights w_i we can write ensemble average of $\mathcal{O}$ as

$$\langle\langle \mathcal{O} \rangle\rangle \equiv \sum_i w_i \langle \Psi_i | \mathcal{O} | \Psi_i \rangle \tag{2.6}$$

Now using a more general complete basis $\{|\alpha_i\rangle\}$ in Hilbert space we can write

$$\begin{aligned}
\langle\langle \mathcal{O} \rangle\rangle &= \sum_i w_i \sum_{j,k} \langle \Psi_i | \alpha_j \rangle \langle \alpha_j | \mathcal{O} | \alpha_k \rangle \langle \alpha_k | \Psi_i \rangle \\
&= \sum_{j,k} \langle \alpha_k | \left(\sum_i w_i |\Psi_i\rangle\langle\Psi_i| \right) |\alpha_j\rangle \langle \alpha_j | \mathcal{O} | \alpha_k \rangle \\
&= \sum_{j,k} \langle \alpha_k | \rho | \alpha_j \rangle \langle \alpha_j | \mathcal{O} | \alpha_k \rangle \\
&= \mathrm{Tr}(\rho \mathcal{O})
\end{aligned}$$

where the density matrix defined as $\rho = \sum_i w_i |\Psi_i\rangle\langle\Psi_i|$. Since the statistical weights satisfy the normalization condition, density matrix also satisfies $\mathrm{Tr}(\rho) = 1$. In case

of a pure state, one of the weights can be considered as one and others become zero, and $\rho^2 = \rho$ with $\mathrm{Tr}(\rho^2) = 1$. For a mixed state, $\rho^2 \neq \rho$ and $\mathrm{Tr}(\rho^2) < 1$. The time dependent form of the density matrix can be written as $\rho(t) = \sum_i w_i |\Psi_i, t\rangle\langle\Psi_j, t|$. We can easily find the equation of motion for the density matrix using Eq. 2.3 as

$$\begin{aligned}\frac{d}{dt}\rho(t) &= \sum_i w_i \left(\frac{\partial}{\partial t}(|\Psi_i, t\rangle)\langle\Psi_i, t| + |\Psi_i, t\rangle\frac{\partial}{\partial t}(\langle\Psi_i, t|)\right) \\ &= i\sum_i w_i \left(-H|\Psi_i, t\rangle\langle\Psi_i, t| + |\Psi_i, t\rangle\langle\Psi_i, t|H\right) \\ &= -i[H, \rho]\end{aligned}$$

which is known as Liouville von Neumann equation and it describes the time evolution of density matrix for isolated statistical quantum systems.

Instead of describing the dynamics using density matrix one can also consider the time evolution of the observables. Schrödinger picture operators are related with Heisenberg picture by the canonical transformation

$$\mathcal{O}_H(t) = U^\dagger(t, t_0)\mathcal{O}(t)U(t, t_0) \tag{2.7}$$

Taking the time derivative for both sides of the equation will give us the Heisenberg equation of motion as

$$\frac{d}{dt}\mathcal{O}_H(t) = i[H_H(t), \mathcal{O}_H(t)] + \frac{\partial\mathcal{O}(t)}{\partial t} \tag{2.8}$$

Since the evolution is unitary expectation value of an observable will be same for both pictures. If it is time independent $\mathcal{O}_H$ will be constant of motion.

The more general description of the dynamics is known as interaction picture. The Hamiltonian can be written as time independent and dependent parts as

$$H(t) = H_0 + H_I(t) \tag{2.9}$$

We can define the evolution operator only considering time independent part of the Hamiltonian

$$U_0(t, t_0) = e^{-iH_0(t-t_0)} \tag{2.10}$$

If we consider the density matrix the system as $\rho(t)$, in the interaction picture it will be $\tilde{\rho}(t) = U_0^\dagger(t,t_0)\rho(t)U_0(t,t_0)$. Then interaction Hamiltonian in this picture is going to be $\tilde{H}_I(t) = U_0^\dagger(t,t_0)H_I(t)U_0(t,t_0)$. We can easily find the corresponding von Neumann equation in the interaction picture as

$$\frac{d}{dt}\tilde{\rho}(t) = -i[\tilde{H}_I, \tilde{\rho}(t)] \tag{2.11}$$

One can easily write the integral form of the von Neumann equation in this picture as

$$\tilde{\rho}(t) = \tilde{\rho}(t_0) - i\int_{t_0}^{t} dt'[\tilde{H}_I(t'), \tilde{\rho}(t')] \tag{2.12}$$

Integral form of this equation is important dealing with the open quantum system and perturbative systems which we will describe in the following sections.

2.2 Entropy of Quantum Systems

2.2.1 von Neumann Entropy

Entropy can be identified as a quantitave disorder of the system. For a given density matrix, entropy of quantum state can be found from von Neumann entropy, which is defined as

$$S(\rho) = -\mathrm{Tr}(\rho \ln \rho). \tag{2.13}$$

where, one needs to include Boltzmann constant k_B for definition of entropy in statistical quantum mechanics, here I will take it as 1 for simplicity. Now considering eigendecomposition of the density matrix as

$$\rho = \sum_i p_i |\Psi_i\rangle\langle\Psi_i|, \tag{2.14}$$

where $\sum_i p_i = 1$, we can find

$$S(\rho) = -\sum_i p_i \ln p_i \equiv H(p_i). \tag{2.15}$$

which is equivalent to Shannon entropy $H(p_i)$ [59]. We can summarize some important properties of von-Neumann entropy as following;

i $S(\rho) \geq 0$, where it can be zero only for pure states.

ii $S(\rho) \leq N$, for a Hilbert space with dimension N, equality only holds for maximally mixed states.

iii $S(\rho)$ is invariant under any unitary transformation $S(\rho) = S(U\rho U^{\dagger})$ because of the cyclic property of trace.

iv Subadditivity condition; if a composite system with ρ in a Hilbert space $\mathcal{H} = \mathcal{H}_A \otimes \mathcal{H}_B$ and $\rho_A = \mathrm{Tr}_B[\rho], \quad \rho_B = \mathrm{Tr}_A[\rho]$ then they satisfy the inequality in the form $S(\rho) \leq S(\rho_A) + S(\rho_B)$.

2.2.2 Relative Entropy

The relative entropy can be considered to distinguish the quantum states. It can be seen as a distance measure between two density matrices of a quantum system. Considering two pair of ρ and σ as density matrices we can write the relative entropy as

$$S(\rho||\sigma) = \mathrm{Tr}[\rho \ln(\rho)] - \mathrm{Tr}[\rho \ln(\sigma)] \tag{2.16}$$

We can list the various useful properties of relative entropy;

i $S(\rho||\sigma) \geq 0$, where it can be zero only for $\rho = \sigma$.

ii $S(\rho||\sigma)$ is invariant under any unitary transformation; $S(\rho||\sigma) = S(U\rho U^{\dagger}||U\sigma U^{\dagger})$.

iii If we have a subsystem A and B. Taking a trace over subsystem in both pair of density matrices reduces the relative entropy $\rho_A = \mathrm{Tr}_B[\rho], \quad \sigma_A = \mathrm{Tr}_B[\sigma]$; $S(\rho_A||\sigma_A) \leq S(\rho||\sigma)$ and equality holds for uncorrelated states.

2.3 Open Quantum Systems

Let's first consider a combined total system as a isolated (closed) quantum system. In this combined system we have a reduced system and reservoir. We can denote Hilbert space of the subsystem by $\mathcal{H}_{\mathrm{S}}$ and reservoir by $\mathcal{H}_B$. For total system, the Hilbert space is just a tensor product of these two spaces$\mathcal{H} = \mathcal{H}_{\mathrm{S}} \otimes \mathcal{H}_B$. The dynamics of this isolated system is described by the von-Neumann equation [59].

$$\frac{d}{dt}\rho(t) = -i[H(t), \rho(t)] \equiv \mathcal{L}_{\mathrm{tot}}(t)\rho(t) \tag{2.17}$$

Here, $\mathcal{L}_{\mathrm{tot}}$ is the Liouville super-operator. It acts on an operator and gives you an other operator. The total system may be written as

$$H(t) = H_{\mathrm{S}} + H_B + H_I(t) \tag{2.18}$$

where, $H_I(t)$ is the interaction between reduce system and the reservoir. At $t = 0$ we can write initial density matrix of the total system as tensor product of density matrix of subsystem $\rho_{\mathrm{S}}(0)$ and reservoir ρ_B as $\rho(0) = \rho_{\mathrm{S}}(0) \otimes \rho_B$. Now, considering the state of the reservoir ρ_B is fixed reference state which is not time dependent. The evolution of reduced system can be found in two ways. One way of this is that taking partial trace of total system after unitary evolution. The other one is using a dynamical map.

2.3.1 Dynamical Semigroup

In this part, we are going to approximate this equation under the condition of the short reservoir and reduced system correlation [59–61]. We will not care about the memory effect. Then, we will show the system dynamics in terms of the quantum dynamical semigroup [62, 63]. The term semigroup means that the evolution of time forms a family of maps but it does not contain the negative range of parameter time. Thus, the inverse property of the group is missing. In the physical point of view, it is the property of irreversible dynamics. So, this allows us to distinguish the past from future. A dynamical map $\Lambda(t)$ describes the state change of the reduced system. It

is a map between C^*-algebras that maps a linear positive operator O into a linear positive operator [64]. This family of maps $\{\Lambda(t), t \geq 0\}$ are satify these properties;

i At t=0 map is identity; $\Lambda(0) = 1$

ii Completely positive ; The dynamial map preserves the positivity regarding the tensor product operations.

iii Trace preserving ; $\mathrm{Tr_S}(\Lambda(t)\rho_\mathrm{S}) = \mathrm{Tr_S}\rho_\mathrm{S} = 1$

iv Markovian (memoriless) ; $\Lambda(t_1 + t_2) = \Lambda(t_1)\Lambda(t_2)\ t_1, t_2 \geq 0$

v Strongly continuous property ; $\lim \parallel \Lambda(t)X - X \parallel$ for $\forall X \in B$. X is a linear bounded operator.

vi Contraction semigroup property ; $\parallel \Lambda(t) \parallel \leq 1$

Now, based on these mathematical properties, we can define a generator$\mathcal{L}$ of this dynamical semigroup as

$$\Lambda(t) = e^{\mathcal{L}t}$$

and

$$\frac{d}{dt}\rho_\mathrm{S}(t) = \mathcal{L}\rho_\mathrm{S}(t)$$

which is named as Markovian master equation where, $\mathcal{L}$ is called the super operator. The general form of $\mathcal{L}$ can be found in finite dimensional Hilbert space $\mathcal{H}_\mathrm{S}$, $dim(\mathcal{H}_\mathrm{S}) = N$. Then, the dimension of Liouville space will be N^2 complex space. The spectral decomposition of the density matrix of reservoir can be written as

$$\rho_B = \sum_i \lambda_i \left|\varphi_i\right\rangle \left\langle\varphi_i\right| \tag{2.19}$$

And, we can express propagator as;

$$U(t,0) = \sum_{i,j} A_{ij} \otimes \left|\varphi_i\right\rangle \left\langle\varphi_i\right| \tag{2.20}$$

Here, A_{ij} are operators acting on the reduced system. Using this propagator $\rho_S(t)$ becomes

$$\rho_S(t) = \Lambda(t)\rho_S(0) = \sum_n K_n \rho_S(0) K_n^\dagger \tag{2.21}$$

$K_n := \sqrt{\lambda_j} A_{ij}(t,0)$ defined as Kraus operator and $\sum_n K_n K_n^\dagger = 1$. Introducing new set of orthonormal operators $\{V_k, k = 1, ..., N^2 - 1\}$ we can write simpler form of generator as

$$\frac{d}{dt}\rho_S = -i[H, \rho_S] + \sum_{k=1}^{N^2-1} \gamma_k (V_k \rho_S V_k^\dagger - \frac{1}{2}\{V_k^\dagger V_k, \rho_S\}) \quad = -i[H, \rho_S] + \mathcal{L}_D \tag{2.22}$$

$\mathcal{L}_D$ is the dissapative part of $\mathcal{L}$. This is the most general form of the Markovian master equation in Schrödinger picture. V_k known as the Lindbad operators. γ_k have the dimension inverse of time. They are given in terms of certain correlation function of the reservoir, also they are related with the relaxiation rates for different decay modes of the open quantum systems. From this Schrödinger picture Lindblad generator we can go to Heisenberg picture Lindblad generator. The Heisenberg picture dynamical map can be written as $\Lambda^\dagger(t)$ and it acts on operators $\mathcal{O}$ in the Hilbert space of the reduced system $\mathcal{O}_H = \Lambda^\dagger(t)\mathcal{O}$. Since;

$$\mathrm{Tr}(\mathcal{O}\Lambda(t,0)\rho_S) = \mathrm{Tr}(\Lambda^\dagger(t,0)\mathcal{O}\rho_S) \tag{2.23}$$

The adjoint propagator;

$$\Lambda^\dagger(t, t_0) = \mathcal{T} e^{\int_{t_0}^t ds \mathcal{L}^\dagger(s)} \tag{2.24}$$

will satify

$$\frac{\partial}{\partial t}\Lambda^\dagger(t, t_0) = \Lambda^\dagger(t, t_0)\mathcal{L}^\dagger(t) \tag{2.25}$$

This equation known as the adjoint master equation. If $[\mathcal{L}^\dagger, \Lambda^\dagger] = 0$ then it is reduced to ;

$$\frac{d}{dt}\mathcal{O}_H = \mathcal{L}^\dagger \mathcal{O}_H(t) = i[H, \mathcal{O}_H] + \sum_{k=1}^{N^2-1} \gamma_k (V_k^\dagger \mathcal{O}_H V_k - \frac{1}{2}\{V_k V_k^\dagger, \mathcal{O}_H\}) + \frac{\partial}{\partial t}\mathcal{O}_H \tag{2.26}$$

This equation is the Heisenberg picture Lindblad generator.

2.3.2 Quantum Description of Spin-Lattice Relaxation of the NMR system

The relaxation theory of NMR systems studied deeply in the literature [65–68]. Here, in this thesis I will just give how we can derive quantum description of longitudinal relaxation of NMR following the M.Goldman notes [69]. In the case of NMR, we are considering the quantum system in a lattice kind of environment [49]. The relaxation mechanism of the NMR systems rely on both system and lattice variables. And without interaction between spin and lattice Hamiltonian for such a system in the form of $H_0 = H_{\rm S} + H_{\rm L}$, with interaction $H = H_0 + H_I$. Where $H_{\rm S}$ and $H_{\rm L}$ are the spin and the lattice Hamiltonians respectively and H_I is the interaction term between them. The dynamics of the density matrix describing the whole system is given by the von-Neumann equation (see Eq. 2.17). Assuming that the coupling between the system and the lattice is weak (Born Approximation) one can write $\rho = \rho_{\rm S} \otimes \rho_{\rm L}$. Here, $\rho_{\rm S}$ is the system density matrix and $\rho_{\rm L}$ is the lattice environment density matrix. Also, we are assuming the density matrix of the lattice environment does not depend on time. The equilibrium state characterized by a temperature $T_{\rm L}$ can be written as

$$\rho_{\rm L} = \frac{e^{-\beta_{\rm L} H_{\rm L}}}{{\rm Tr}(e^{-\beta_{\rm L} H_{\rm L}})} \tag{2.27}$$

where $\beta = \hbar/k_B T_{\rm L}$. One can consider the system Hamiltonian is static (does not depend on time). In the absence of H_I, the unitary evolution operator for evolution can be found as

$$U(t) = e^{-iH_0 t} = e^{-i(H_{\rm S}+H_{\rm L})t} \tag{2.28}$$

In the interaction representation we can single out the effect of H_I. Then density matrix of total system will be in the form

$$\frac{d}{dt}\tilde{\rho}(t) = -i[\tilde{H}_I(t), \tilde{\rho}(t)] \tag{2.29}$$

where $\tilde{\rho}(t) = e^{iH_0 t}\rho e^{-iH_0 t}$ and $\tilde{H}_I(t) = e^{iH_0 t} H_I e^{-iH_0 t}$. Total density matrix $\tilde{\rho}(t)$ in its integral form can be written as

$$\tilde{\rho}(t) = \tilde{\rho}(0) - i\int_0^t ds[\tilde{H}_I(s), \tilde{\rho}(s)] \tag{2.30}$$

which yields the equation in the dynamical form

$$\frac{d}{dt}\tilde{\rho}(t) = -i[\tilde{H}_I, \tilde{\rho}(0)] - \int_0^t ds[\tilde{H}_I(t), [\tilde{H}_I(s), \tilde{\rho}(s)]] \tag{2.31}$$

Also we can just assume $[\tilde{H}_I, \tilde{\rho}(0)] = 0$ by taking the ensemble average. Here I will make further assumptions as follows

- The evolution time t for the $\tilde{\rho}(t)$ is much longer than the correlation time τ_C of the environment. This assumption yields to upper bound of the integral in Eq. 2.31 to infinity.

- We have a decoupling term between spin and lattice ensemble averages. This may lead us to change $\tilde{\rho}(s)$ to $\tilde{\rho}(t)$ in the integral (Markov Approximation).

Under these assumptions we can go back Schrödinger representation by inverting $\tilde{\rho}(t)$ as $\rho(t) = e^{-iH_0t}\tilde{\rho}(t)e^{iH_0t}$ and by differentiating both sides, we can write Eq 2.31 in the form as

$$\frac{d}{dt}\rho(t) = -i[H_0, \rho(t)] - \int_0^\infty d\tau[H_I, [\tilde{H}_I(-\tau), \rho(t)]] \tag{2.32}$$

Here, re-defining the following terms as $\tilde{H}_I(-\tau) \equiv \hat{H}_I(\tau) = e^{-iH_0\tau}H_Ie^{iH_0\tau}$, we can write

$$\frac{d}{dt}\rho(t) = -i[H_0, \rho(t)] - \int_0^\infty d\tau[H_I, [\hat{H}_I(\tau), \rho(t)]] \tag{2.33}$$

Interaction Hamiltonian in the Schrödinger picture can be written as $H_I = \sum_\alpha A_\alpha F_\alpha$, where A_α are system operators and chosen to be in relation as $[H_\mathrm{S}, A_\alpha] = \omega_\alpha A_\alpha$. And F_α are time-independent lattice operators. Time-dependent form of these operators can be written as $\hat{A}^\dagger_\alpha(\tau) = e^{-iH_\mathrm{S}\tau}A^\dagger_\alpha e^{iH_\mathrm{S}\tau} = e^{i\omega_\alpha\tau}A^\dagger_\alpha$ and, $\hat{F}^\dagger_\alpha(\tau) = e^{-iH_\mathrm{L}\tau}F^\dagger_\alpha e^{iH_\mathrm{L}\tau}$. Then the dynamical equation becomes

$$\frac{d}{dt}\rho(t) = -i[H_0, \rho_\mathrm{S} \otimes \rho_\mathrm{L}] - \sum_{\alpha,\beta}\int_0^\infty d\tau[A_\alpha F_\alpha, [\hat{A}^\dagger_\beta(\tau)\hat{F}^\dagger_\beta(\tau), \rho_\mathrm{S} \otimes \rho_\mathrm{L}]] \tag{2.34}$$

Just for simplicity for calculations lets write these operators $A_\alpha = A$, $\hat{A}^\dagger_\beta(\tau) = \hat{A}$, $\hat{F}^\dagger_\beta(\tau) = \hat{F}$ and $F_\alpha = F$. Then the equation for total density matrix can be written

as

$$\frac{d}{dt}\rho(t) = -i[H_0, \rho_S \otimes \rho_L] - \int_0^\infty d\tau [AF, [\hat{A}(\tau)\hat{F}(\tau), \rho_S \otimes \rho_L]] \tag{2.35}$$

Using procedure above; taking partial trace over lattice variables in Eq 2.35, then dynamical equation for the system density matrix becomes

$$\frac{d}{dt}\rho_S(t) = -i\mathrm{Tr}_L([H_0, \rho_S \otimes \rho_L]) - \mathrm{Tr}_L\left(\int_0^\infty d\tau [AF, [\hat{A}(\tau)\hat{F}(\tau), \rho_S \otimes \rho_L]]\right) \tag{2.36}$$

Dealing with commutation and partial trace as follows

$$\mathrm{Tr}_L([H_0, \rho_S \otimes \rho_L]) = [H_S, \rho_S] \tag{2.37}$$

Then the trace in the integral can be written easily as

$$\mathrm{Tr}_L(AF, [\hat{A}(\tau)\hat{F}(\tau), \rho_S \otimes \rho_L]) = [A, \hat{A}\rho_S]\mathrm{Tr}_L([\hat{F}, \rho_L]F]) + [A, [\hat{A}, \rho_S]]\mathrm{Tr}_L(\rho_L \hat{F} F)$$

We can identify $\mathrm{Tr}_L(\rho_L \hat{F} F)$ as two time correlation function considering initially at $t = 0$ as $F = \hat{F}(0)$.

$$\mathrm{Tr}_L(\rho_L \hat{F} F) = \langle \hat{F}_\alpha^\dagger(\tau)\hat{F}_\beta(0)\rangle \tag{2.38}$$

Then the first trace in the equation can be calculated as

$$\mathrm{Tr}_L([\hat{F}, \rho_L]F) = \sum_{f,f'}(\langle f|\,\rho_L\,|f\rangle\,\langle f|\,\hat{F}\,|f'\rangle\,\langle f'|\,F\,|f\rangle)) \times \left(\frac{\langle f'|\,\rho_L\,|f'\rangle}{\langle f|\,\rho_L\,|f\rangle} - 1\right), \tag{2.39}$$

and using the definition of ρ_L as a thermal state, the ratio in the equation can be found as

$$\frac{\langle f'|\,\rho_L\,|f'\rangle}{\langle f|\,\rho_L\,|f\rangle} = e^{\beta_L(\omega_f - \omega_{f'})} \tag{2.40}$$

Using the definitions of $\hat{F}$, and $\hat{A}$ given as earlier, we can find the following relations as $\langle f|\,\hat{F}\,|f'\rangle = e^{-i(\omega_f - \omega_{f'})\tau}\,\langle f|\,F_\beta^\dagger\,|f'\rangle$, and $\hat{A}_\beta^\dagger(\tau) = e^{i\omega_\beta \tau}A_\beta^\dagger$. And these lead to an integral as

$$\int_0^\infty e^{i(\omega_\beta - \omega_f + \omega_{f'})\tau} d\tau \propto \delta(\omega_\beta - \omega_f + \omega_{f'}) \tag{2.41}$$

We can change $\omega_f - \omega_{f'}$ in Eq. 2.40 with ω_β. After substituting all relations to Eq 2.35. We can find the master equation for system as

$$\frac{d}{dt}\rho_{\rm S}(t) = -i[H_{\rm S}, \rho_{\rm S}] - \sum_{\alpha,\beta} J_{\alpha,\beta}(\omega_\beta) \Big(([A_\alpha, [A_\beta^\dagger, \rho_{\rm S}]] - [A_\alpha, A_\alpha^\dagger \rho_{\rm S}](1 - e^{\beta_{\rm L}\omega_\beta}) \Big) \quad (2.42)$$

where $J_{\alpha,\beta}(\omega_\beta)$ is the spectral density function can be written as

$$J_{\alpha,\beta}(\omega_\beta) = \int_0^\infty d\tau e^{i\omega_\beta \tau} \langle \hat{F}_\alpha^\dagger(\tau) \hat{F}_\beta(0) \rangle \quad (2.43)$$

The evolution of the observables of the system are can be found from the operators expectation values $\langle Q \rangle = {\rm Tr}(Q\rho_{\rm S})$, and using the Eq. 2.42 one can write $\frac{d}{dt}\langle Q \rangle = {\rm Tr}(Q \frac{d}{dt}\rho_{\rm S})$. The general property of trace (${\rm Tr}(A[B,C]) = {\rm Tr}([A,B]C])$) allow us to find Eq. 2.42 in the operator form as

$$\frac{d}{dt}\langle Q \rangle(t) = -i[Q, H_{\rm S}] - \sum_{\alpha,\beta} J_{\alpha,\beta}(\omega_\beta) \Big((\langle [Q, A_\alpha] A_\beta^\dagger] \rangle - \langle [Q, A_\alpha] A_\beta^\dagger \rangle (1 - e^{\beta_{\rm L}\omega_\beta}) \Big) \quad (2.44)$$

Example; Two Level System Couples with Lattice Environment

To give the basic example we can consider single spin 1/2 system coupled with a thermal lattice environment.

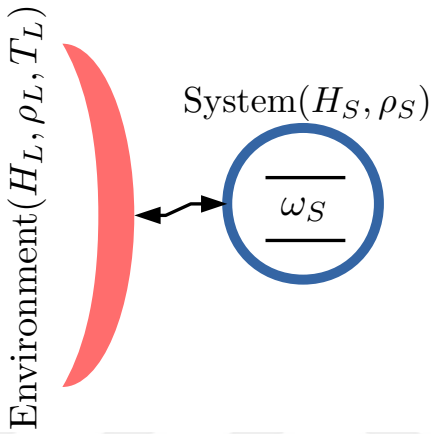

H_{S} is the Hamiltonian for the two-level system and ρ_{S} the general form of the density matrix of the system. In NMR it is more often to use I_z instead of σ_z (Pauli operator). Then Hamiltonian can be written as $H_{\mathrm{S}} = -\omega_{\mathrm{S}} I_z$, where $\omega_{\mathcal{S}}$ is the characteristic frequency of the system. Using the relations $[H_{\mathrm{S}}, I_+] = -\omega_{\mathrm{S}} I_+$, $[H_{\mathrm{S}}, I_-] = \omega_{\mathrm{S}} I_-$, and $[H_{\mathrm{S}}, I_z] = 0$. We can identify operators for quantum master equation in Eq 2.44 as $\{I_+, I_-, I_z\}$. The interaction Hamiltonian between the lattice environment and system can be written as $H_I = I_+ F + I_- F^\dagger$. Using the master equation in the operator form that we found in Eq. 2.44 for $\langle I_z \rangle$ we can write

$$\begin{aligned}\frac{d}{dt}\langle I_z\rangle(t) = &-J(-\omega_{\mathrm{S}})\left(\left(\langle[I_z, I_+], I_-]\rangle - \langle[I_z, I_+]I_-\rangle(1 - e^{-\beta_{\mathrm{L}}\omega_{\mathrm{S}}})\right)\right.\\ &\left. - J^\dagger(\omega_{\mathrm{S}})\left(\left(\langle[I_z, I_-], I_+]\rangle - \langle[I_z, I_-]I_+\rangle(1 - e^{\beta_{\mathrm{L}}\omega_{\mathrm{S}}})\right)\right.\end{aligned}$$

Here, $-i[I_z, H_{\mathrm{S}}] = 0$, $J^\dagger(\omega_{\mathcal{S}}) = J(-\omega_{\mathcal{S}})e^{-\beta_{\mathrm{L}}\omega_{\mathcal{S}}}$ and using the following commutation relations

$$\begin{aligned}[I_z, I_-]I_+ &= -\frac{1}{2} + I_z\\ [I_z, I_+]I_- &= \frac{1}{2} + I_z\\ [[I_z, I_+], I_-] &= 2I_z\end{aligned}$$

Then master equation will simplify to form

$$\frac{d}{dt}\langle I_z\rangle(t) = -J(-\omega_{\mathcal{S}})\left(2(e^{\beta_{\mathrm{L}}\omega_{\mathcal{S}}}+1)\langle I_z\rangle - e^{\beta_{\mathrm{L}}\omega}+1\right) \tag{2.45}$$

$$= -2J(-\omega_{\mathcal{S}})(e^{\beta_{\mathrm{L}}\omega_{\mathcal{S}}}+1)\left(\langle I_z\rangle - \frac{1}{2}\tanh\frac{\beta_{\mathrm{L}}\omega_{\mathcal{S}}}{2}\right) \tag{2.46}$$

We can define $-2J(-\omega_{\mathcal{S}})(e^{\beta_{\mathrm{L}}\omega_{\mathcal{S}}}+1)$ as the longiditional relaxation time τ_1 for the NMR two level system. Then, this equation can be fitted to experimental values. At equilibrium with the lattice environment, the left hand side of the equation will vanish then we have $I_z\rangle^{eq}$. Then simpler form of the equation can be written as

$$\frac{d}{dt}\langle I_z\rangle(t) = -\frac{1}{\tau_1}\left(\langle I_z\rangle - \langle I_z\rangle^{eq}\right), \qquad \langle I_z\rangle^{eq} = \frac{1}{2}\tanh\left(\frac{\beta\omega_{\mathcal{S}}}{2}\right) \tag{2.47}$$

which is consistent with the general result of the Gibbs state. Now we introduce the spin polarization due to quantization axes z. Considering $I_z = \sigma_z/2$ we can define the spin polarization as

$$\epsilon_{\mathcal{S}} = \tanh\left(\frac{\beta\omega_{\mathcal{S}}}{2}\right) \tag{2.48}$$

2.3.3 Quantum Thermodynamics

In quantum thermodynamics an equilibrium state is defined as stationary and stable. In equilibrium there no energy flow between system and bath. This is known as Kubo-Martin-Schwinger stability condition and it implies the zeroth law for a network of coupled systems. The first law of thermodynamics related with conservation of energy [70–72]. If a system is closed and no energy source, then the energy is conserved. This means that total energy of the closed system is constant. $\langle H\rangle = const.$ and energy of the reduced system can be written as $\langle H_{\mathrm{S}}\rangle = E_{\mathrm{S}} = \mathrm{Tr}(\rho_{\mathrm{S}}H_{\mathrm{S}})$ The time derivative of the system's energy becomes

$$\frac{d}{dt}E_{\mathrm{S}} = \mathrm{Tr}\left(\frac{d\rho_{\mathrm{S}}}{dt}H_{\mathrm{S}}\right) + \mathrm{Tr}\left(\rho_{\mathrm{S}}\frac{dH_{\mathrm{S}}}{dt}\right) \tag{2.49}$$

Here, first and second therm can be identified as heat current and power. Also, using Heisenberg picture master equation it can be written as [73, 74];

$$\begin{aligned}\frac{d}{dt}E_{\mathrm{S}} &= \langle\frac{\partial H_{\mathrm{S}}}{\partial t}\rangle + \langle\mathcal{L}_D\rangle \\ &= \mathcal{P} + \sum_{j}^{N}\mathcal{J}_j\end{aligned}$$

Quantum thermodynamics deals with the balance of energy of the system. Here

$$\mathcal{P} := \langle\frac{\partial H_{\mathrm{S}}}{\partial t}\rangle \tag{2.50}$$

external power. And

$$\mathcal{J}_j := \langle V_j H_{\mathrm{S}} V_j^{\dagger} - \frac{1}{2}\{V_j V_j^{\dagger}, H_{\mathrm{S}}\}\rangle \tag{2.51}$$

Heat current from j th bath. This is the dynamical version of the first law.

The second law of thermodynamics is related with irreversibility of dynamics which states that heat will flow spontaneously from a hot bath to a cold bath and change in entropy of closed system is positive: $\Delta S \geq 0$. The quantum Markovian master equation describes the irreversible evolution of open quantum system. To describe irreversible character of the quantum dynamical semigroup let's investigate the change of the relative entropy $S(\rho \parallel \rho_0)$ of two reduced system ρ and ρ_0 considering an dynamical map $\Lambda(t)$.

$$\begin{aligned}S(\Lambda(t)\rho \parallel \Lambda(t)\rho_0) &= S\left(\mathrm{tr}\{U(t,0)\rho\otimes\rho_B U^{\dagger}(t,0)\} \parallel \mathrm{tr}\{U(t,0)\rho_0\otimes\rho_B U^{\dagger}(t,0)\}\right) \\ &\leq S\left(U(t,0)\rho\otimes\rho_B U^{\dagger}(t,0)\} \parallel U(t,0)\rho_0\otimes\rho_B U^{\dagger}(t,0)\right) \\ &\leq S(\rho \parallel \rho_0)\end{aligned}$$

If we chose ρ_0 to be stationary, $\Lambda(t)\rho_0 = \rho_0$. Then;

$$S(\Lambda(t)\rho \parallel \rho_0) \leq S(\rho \parallel \rho_0) \tag{2.52}$$

Since, it is a dynamical semigroup; using the semigroup property we can say that the negatif time derivative of $S(\rho \parallel \rho_0)$ is always positive or zero.

$$\sigma(\rho(t)) = -\frac{dS(\rho \parallel \rho_0)}{dt} \geq 0 \tag{2.53}$$

Here, $\sigma(\rho(t))$ called entropy production and it is positive or zero. Then, using definition of relative entropy $S(\rho \parallel \rho_0) \equiv \mathrm{Tr}[\rho(\ln \rho - \ln \rho_0)]$ one can find;

$$\sigma(\rho(t)) = -\mathrm{Tr}[\mathcal{L}(\rho)(\ln \rho - \ln \rho_0)] \geq 0 \tag{2.54}$$

which is known as Spohn's inequality [75]. Lets first consider a simple network a system couple with two heat bath cold and hot[73]. J_h is the heat current from hot bath with temperature T_h and J_c is the heat current from cold bath with temperature T_c. And $-\frac{J_c}{T_c} - \frac{J_h}{T_h} \geq 0$. If we generalize it to the N heat bath. It will be;

$$-\sum_j^N \frac{J_j}{T_j} \geq 0 \tag{2.55}$$

Thus, in steady state second law will be in this form. In non equlibrium thermodynamics the entropy obeys a balance equation, taking time derivative of von-Neumann entropy and using Spohn's inequality one can obtain as a dynamical version of the second law;

$$\sigma(\rho) = \frac{dS(\rho)}{dt} - \sum_j^N \frac{J_j(t)}{T_j} \geq 0 \tag{2.56}$$

2.3.4 Quantum Isothermal Process

The quantum Isothermal process can be used in quantum Carnot engines. We will just briefly explain the process and we will not give detail about Carnot engines in this thesis. But one can see these references for the detail [5]. In the isothermal process, the quantum system in a thermal environment must be kept in a thermal equilibrium state. During the process, energy levels and the occupation probabilities are changing simultaneously while keeping the system in a thermal equilibrium state. The quantum system can perform work to the thermal environment and exchange heat under the isothermal process. At every instant of time, the process should be slow enough to stay in equilibrium.

2.3.5 Quantum Isochoric Process

In the quantum isochoric process, the model of the quantum system connected with a thermal environment [18]. The heat exchange between the quantum system and thermal equilibrium is provided by the open quantum system dynamics given in Sec. 2.3.2. During the process, the quantum system approaches an equilibrium state with a thermal environment. At the end of the process, we can assume that the system is in a thermal equilibrium state with the heat bath. The occupation probabilities and eventually the von Neumann entropy of the system are going to change during the process. So, there is only heat exchange between the thermal environment and the quantum system. Moreover, the corresponding eigen energies of the system kept invariant as a result no work is done in the quantum isochoric process.

2.3.6 Quantum Adiabatic Process

For a quantum adiabatic process, a quantum system is isolated and the Hamiltonian of the system externally controlled by time-dependent drive Hamiltonian $H_{drive}(t)$. In the process, total Hamiltonian can be written as $H(t) = H_0 + H_{drive}(t)$. Since the quantum system is isolated from environment dynamics is unitary. Therefore, the von Neumann entropy of the system is invariant under the process. Also, the information entropy does not change during the process. These restrictions bring a result; during the process, the occupation probabilities of the system should stay the same. In the processes there is no heat exchange, there is only work output. Thus, Hamiltonian in different times needs to commute; $[H(t), H(t')] = 0$. If it is not commute, then there will be internal friction in the system and it causes the occupation probabilities to change. To approximate adiabatic dynamics, process should be very slow. However, even if the Hamiltonian does not commute, because of the unitary dynamics system may be recovered by external work.

2.4 Quantum Information Processing

The two-level system is the simplest system in quantum mechanics. It represents many physical systems such as electrons, protons, photons and any spin 1/2 dynamics. In addition to this, it carries binary information. Considering the similarity between classical information theory in the concept of bits like 0 and 1, and quantum information theory, the two-level system is called quantum-bit (qubit) [47, 76, 77]. Basis of the system can be represented with Dirac notation with $|0\rangle$ and $|1\rangle$ as

$$|0\rangle = \begin{bmatrix} 1 \\ 0 \end{bmatrix}, \quad |1\rangle = \begin{bmatrix} 0 \\ 1 \end{bmatrix}. \tag{2.57}$$

Unlike the classical information bits, qubits can also be superposition state. The most general form can be written as

$$|\psi\rangle = \cos\left(\frac{\theta}{2}\right)|0\rangle + e^{i\phi}\sin\left(\frac{\theta}{2}\right)|1\rangle \quad \Longrightarrow \tag{2.58}$$

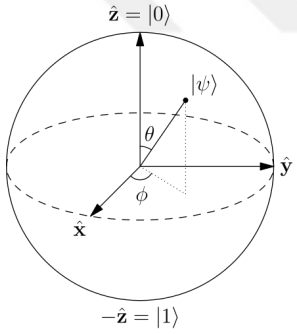

and we can represent it in the Bloch sphere for quantum states. The angles represent a point on the surface of the sphere with radius 1. The transition from one point on the sphere to another is achieved by unitary transformation. In such a system, unitary transformations are represented by rotation of the state vector. This process are called spin rotations. In particular, we cant to calculate $R_i(\theta) = e^{-iI_i\theta}$, where $I_i = \sigma_i/2$ and σ_i 's are the Pauli spin matrices. Using Taylor series expansion we can find

$$R_i(\theta) = \cos\left(\frac{\theta}{2}\right)\mathbb{I} - i\sin\left(\frac{\theta}{2}\right)I_i \tag{2.59}$$

As in classical information theory, there are logic gates in quantum information processing. However, logic gates are reversible operations because of the unitary evolution. There are many logic gates, single or multi-qubit. The simplest examples are

the Pauli gates which are given as;

$$X = \begin{bmatrix} 0 & 1 \\ 1 & 0 \end{bmatrix}, \qquad Y = \begin{bmatrix} 0 & -i \\ i & 0 \end{bmatrix}, \qquad Z = \begin{bmatrix} 1 & 0 \\ 0 & -1 \end{bmatrix}. \tag{2.60}$$

All these gates can apply for single qubit. Here X gate considered as Not gate as analog to classical information theory if the state is $|0\rangle$ it makes flip to $|1\rangle$ or reverse. There is also another important gate can applicable for single qubit known as Hadamard gate

$$H = \begin{bmatrix} 1 & 1 \\ 1 & -1 \end{bmatrix} \implies \tag{2.61}$$

When it is applied to states $|0\rangle$ and $|1\rangle$, it gives a superposition states as

$$H|0\rangle = \frac{|0\rangle + |1\rangle}{\sqrt{2}}, \qquad H|1\rangle = \frac{|0\rangle + |1\rangle}{\sqrt{2}} \tag{2.62}$$

One of the basics gate for two qubits ($|\mathcal{T}\rangle$ and $|\mathcal{R}\rangle$) is the Controlled-Not (CNot) gate. It controls the one of the qubit then applies a X gate to other qubit. Considering composite quantum state as $|\mathcal{TR}\rangle$, CNot gate applied as $\text{CNot}_{\mathcal{T}}|\mathcal{TR}\rangle = |\mathcal{T}, \mathcal{T} \oplus \mathcal{R}\rangle$, where $\oplus$ symbol represents the addition according to mode 2. The CNot gates can be represented as the following

$$\text{CNot}_{\mathcal{T}} = \begin{bmatrix} 1 & 0 & 0 & 0 \\ 0 & 1 & 0 & 0 \\ 0 & 0 & 0 & 1 \\ 0 & 0 & 1 & 0 \end{bmatrix} \implies \tag{2.63}$$

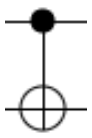

$$\text{CNot}_{\mathcal{R}} = \begin{bmatrix} 1 & 0 & 0 & 0 \\ 0 & 1 & 0 & 1 \\ 0 & 0 & 1 & 0 \\ 0 & 1 & 0 & 0 \end{bmatrix} \implies$$

Another two qubit gate is the SWAP gate. In the case of the composite state $|\mathcal{TR}\rangle$ to which it is applied, it exchanges the states of the qubits to form $\text{SWAP}|\mathcal{TR}\rangle = |\mathcal{RT}\rangle$. SWAP gate can be decompose to three CNot gates as $\text{SWAP} = \text{CNot}_{\mathcal{T}}\text{CNot}_{\mathcal{R}}\text{CNot}_{\mathcal{T}}$. Matrix and circuit representations are given as;

$$\text{SWAP} = \begin{bmatrix} 1 & 0 & 0 & 0 \\ 0 & 0 & 1 & 0 \\ 0 & 1 & 0 & 0 \\ 0 & 0 & 0 & 1 \end{bmatrix} \quad \Longrightarrow \quad  . \tag{2.64}$$

The Toffoli gate is one of three qubit quantum logic gates. Another name is the Control-Control-Not (CCNOT) gate. It can be represented as

$$\text{Toffoli} = \begin{bmatrix} 1 & 0 & 0 & 0 & 0 & 0 & 0 & 0 \\ 0 & 1 & 0 & 0 & 0 & 0 & 0 & 0 \\ 0 & 0 & 1 & 0 & 0 & 0 & 0 & 0 \\ 0 & 0 & 0 & 1 & 0 & 0 & 0 & 0 \\ 0 & 0 & 0 & 0 & 1 & 0 & 0 & 0 \\ 0 & 0 & 0 & 0 & 0 & 1 & 0 & 0 \\ 0 & 0 & 0 & 0 & 0 & 0 & 0 & 1 \\ 0 & 0 & 0 & 0 & 0 & 0 & 1 & 0 \end{bmatrix} \Longrightarrow 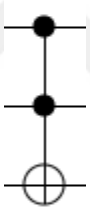 \tag{2.65}$$

Further, the other three qubit gates can be combinations of Control and Not gates as well. One can consider CSWAP gate or Contol-Not-Not gates.

2.5 Heat Bath Algorithmic Cooling

2.5.1 Partner Pairing Algorithm (PPA)

The heat bath algorithmic cooling (HBAC) with partner pairing algorithm (PPA) (see Fig. 2.1) uses quantum information processing to increase the purification level of qubits in NMR systems [4, 36]. Before starting PPA, the individual density matrices

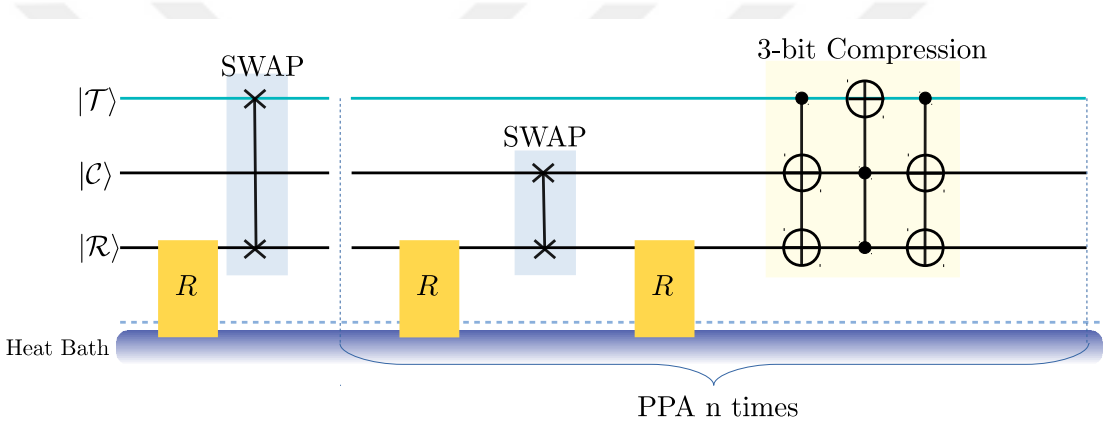

Figure 2.1: Quantum circuit demonstating partner pairing algorithm for 3-qubit system given in Ref. [4]. $|\mathcal{T}\rangle$, $|\mathcal{C}\rangle$ and $|\mathcal{R}\rangle$ stands for target, compression and reset qubits respectively. R process means the relaxation of reset qubit. In PPA, the first reset process applied only one time. Then, the iteration part consists of SWAP and 3-bit compression operations applied n times.

of the target, the compression, and the reset qubits are $\rho_{\mathcal{T}}^{(1)} = \mathrm{Tr}_{\mathcal{C},\mathcal{R}}\left[\rho^{(1)}\right]$, $\rho_{\mathcal{C}}^{(1)} = \mathrm{Tr}_{\mathcal{T},\mathcal{R}}\left[\rho^{(1)}\right]$, $\rho_{\mathcal{R}}^{(1)} = \mathrm{Tr}_{\mathcal{T},\mathcal{C}}\left(\rho^{(1)}\right)$ respectively and $\rho^{(1)}$ is the initial density matrix of three-qubit system. The reset has small relaxation time compared to the target ($\tau_R \ll \tau_T$) and the compression ($\tau_R \ll \tau_C$) qubit, where $\tau_{\mathcal{T}}, \tau_{\mathcal{C}}$ and $\tau_{\mathcal{R}}$ are given in Table 3.1 respectively. In each step of HBAC, R operation is applied to the reset qubit to thermalize it with the heat bath ($\rho_{\mathcal{R}}^{(1)} \rightarrow \rho_{\mathcal{R},th}^{(1)}$) at temperature T. Scalar couplings between qubits are small compared to ω_i values. If we write the total density matrix of three qubits as a tensor product of the individual states, the fidelity of the density matrix in Eq. 3.2 and this product density matrix numerically is found to be close to

1. Thus, at first step, the density matrix of 3-qubit system can be written as a tensor product of these states

$$\rho^{(1,0)} = \rho_{\mathcal{T}}^{(1)} \otimes \rho_{\mathcal{C}}^{(1)} \otimes \rho_{\mathcal{R},th}^{(1)}, \tag{2.66}$$

where, 1st index of $\rho^{(1,0)}$ stands for the stage of the cycle, and 2nd index from 0 to 5 indicates the state after each process of HBAC. After the reset qubit regains its polarization, a unitary SWAP operator is used to exchange polarizations of the target and the reset qubit.

$$\rho^{(1,1)} = \mathrm{SWAP}_{\mathcal{T},\mathcal{R}} \left(\rho^{(1,0)}\right) \mathrm{SWAP}_{\mathcal{T},\mathcal{R}}^{\dagger} \tag{2.67}$$

The states of the target and compression qubits become $\rho_{\mathcal{T}}^{(1,1)} = \mathrm{Tr}_{\mathcal{C},\mathcal{R}} \left[\rho^{(1,1)}\right]$ and $\rho_{C}^{(1,1)} = \mathrm{Tr}_{\mathcal{T},\mathcal{R}} \left[\rho^{(1,1)}\right]$ respectively. After the unitary evolution, PPA can be applied n times, which is given as follows

i The reset qubit is thermalized with the heat bath. The density matrix of the 3-qubit system becomes

$$\rho^{(1,2)} = \rho_{\mathcal{T}}^{(1,1)} \otimes \rho_{\mathcal{C}}^{(1,1)} \otimes \rho_{\mathcal{R},th}^{(1)} \tag{2.68}$$

ii SWAP is applied to change polarization between the compression and the reset qubit, such that

$$\rho^{(1,3)} = \mathrm{SWAP}_{\mathcal{C},\mathcal{R}} \left(\rho^{(1,2)}\right) \mathrm{SWAP}_{\mathcal{C},\mathcal{R}}^{\dagger} \tag{2.69}$$

Then, the states of the target and the compression qubits becomes $\rho_{\mathcal{T}}^{(1,3)} = \mathrm{Tr}_{\mathcal{C},\mathcal{R}} \left[\rho^{(1,3)}\right]$ and $\rho_{C}^{(1,3)} = \mathrm{Tr}_{\mathcal{T},\mathcal{R}} \left[\rho^{(1,3)}\right]$.

iii The reset qubit is regained its polarization. The state of 3-qubit system is expressed as

$$\rho^{(1,4)} = \rho_{\mathcal{T}}^{(1,3)} \otimes \rho_{\mathcal{C}}^{(1,3)} \otimes \rho_{\mathcal{R},th}^{(1)}. \tag{2.70}$$

iv To lower the entropy of the target qubit and to increase the entropy of the reset qubit 3-bit compression gate applied to the density matrix.

$$\rho^{(1,5)} = \mathrm{COMP}\left(\rho^{(1,4)}\right)\mathrm{COMP}^{\dagger} \tag{2.71}$$

where COMP is the unitary operation of compression gate composed of unitary operators as two control-not-not gates and a Toffoli gate, which can be expressed as

$$\mathrm{COMP} = [\mathrm{CNotNot}][\mathrm{Toffoli}][\mathrm{CNotNot}]. \tag{2.72}$$

At the end of this iterative step the target qubit is cooled and the density matrix of it becomes

$$\rho_{\mathcal{T}}^{(2)} = \mathrm{Tr}_{\mathcal{C},\mathcal{R}}\left[\rho^{(1,5)}\right]. \tag{2.73}$$

Chapter 3

FOUR STROKE ALGORITHMIC QUANTUM HEAT ENGINE

3.1 The Working Fluid

Quantum Otto engines (QOEs) consist of quantum adiabatic and isochoric processes [35]. Three types of the quantum heat engine are given in the literature as four-stroke, two-stroke, and continuous [5, 18]. In this thesis, we examined four-stroke, and two-stroke type of QOEs. The basic model of HBAC with PPA is advised instead of isochoric cooling. Implementation of HBAC requires two sets of qubits; reset qubits and computational qubits. One of the computational qubits operated as target qubit which is going to be cooled by applying PPA, while other computational qubits play a role in entropy compression [4]. This cooling process can be implemented with a minimal system composed of just 3-qubit [2–4, 36].

The four-stroke algorithmic heat engine has two adibatic stage, one isochoric stage, and one algorithmic cooling stage. For this engine, we only consider the target qubit as the working fluid (see Fig. 3.1). Reset, and compression qubits are only used in the algorithmic cooling process, and their degrees of freedoms are traced out from the entire state of the system while determining the work output.

In NMR systems, various 3-qubit models have been used for quantum information processing [78–81]. To make an applicable and realistic model for QOEs using these systems, a suitable sample, and a well-designed procedure must be considered. We used parameters of $^{13}C_2$-trichloroethylene (TCE) (see Table 3.1) with paramagnetic reagent $Cr(acac)_3$ in chloroform-d solution ($CDCl_3$) in our numerical calculations, which are also experimentally used for HBAC in Refs. [2, 3]. Carbon-1 and Carbon-2

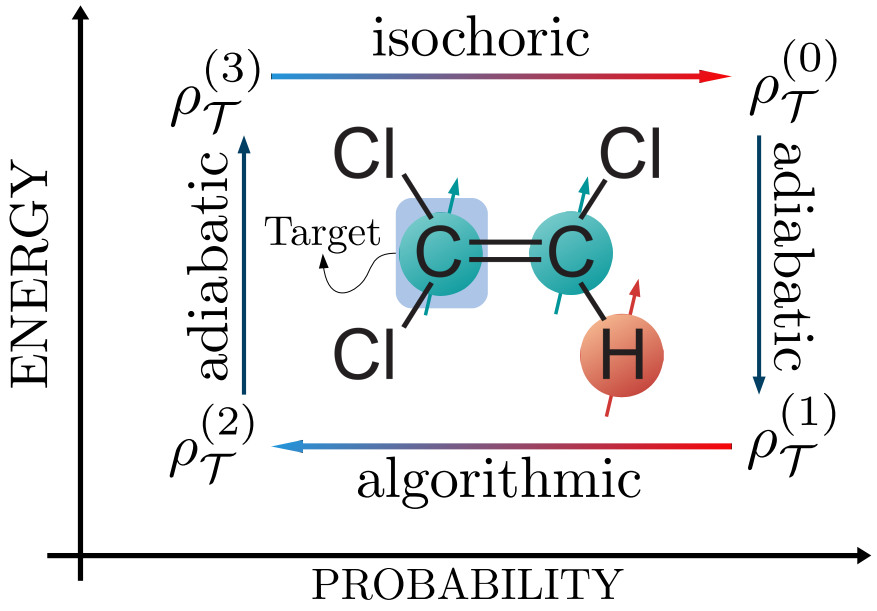

Figure 3.1: (Color online) Four-stroke algorithmic quantum heat engine operating in a single heat bath at temperature T. It has one isochoric heating process, two adiabatic processes and one algorithmic cooling process.

qubits are classified as the target and the compression qubits. Hydrogen qubit is selected as the reset qubit because of the relaxation time, which is small compared to the other two qubits. To implement HBAC, the Hamiltonian of 3-qubit in the lab frame can be written as [47]

$$H^{(0)} = -\hbar \sum_i \omega_i I_{iz} + \hbar \sum_{i \neq j} J_{ij} I_{iz} I_{jz}, \quad i,j = \{\mathcal{T}, \mathcal{C}, \mathcal{R}\}, \tag{3.1}$$

where, $\omega_i = \gamma_i B_z$ is the characteristic frequency of the i^{th} qubit, γ_i is the nuclear gyromagnetic ratio and B_z is the magnetic field. $\mathcal{T}$, $\mathcal{C}$ and $\mathcal{R}$ stand for target, compression and reset qubits, respectively. I_z is the component of the spin angular momentum of the i^{th} qubit and J_{ij} is the scalar isotropic coupling strength between i^{th} and j^{th} qubits. Typically, four-stroke QOEs consist of two isochoric and two adiabatic stages. Instead, we implemented one algorithmic cooling stage instead of one of the isochoric stage (see Fig. 3.1). Adiabatic expansion stage leads to decrease of the level spacing

Table 3.1: The first row in the table shows gyro-magnetic ratio values of Carbon1, Carbon2 and Hydrogen qubits. Regarding the 500 MHz NMR device, the corresponding characteristic frequencies are given in the second row. Also, their experimental τ_1 relaxation times are given in the third row. The last row shows J-coupling strength between these qubits [2, 3].

	Target-**C1**	Compression-**C2**	Reset-**H**
$\gamma/2\pi$	10.7084 [MHz/T]	10.7084 [MHz/T]	42.477 [MHz/T]
$\omega/2\pi$	125.77 [MHz]	125.77 [MHz]	500.13 [MHz]
τ_1	43 [s]	20 [s]	3.5 [s]
	C1-C2	**C1-H**	**C2-H**
$J/2\pi$	103 [Hz]	9 [Hz]	200.8 [Hz]

of the qubits. This happens when the magnetic field decreases. In the opposite case, if the level spacing of the qubits is increasing then we call it as adiabatic compression. This allows for a more faithful representation of the classical Otto cycle terminology for our algorithmic engine. The details of the four-stroke cycle are described as follows.

3.2 Isochoric Heating:

3-qubit of TCE molecule with Hamiltonian in Eq. (3.1) is in contact with a heat bath at temperature $T = 300$ K. The density matrix of the 3-qubit system at the end of this stage is given by thermalized state as

$$\rho_{\text{th}}^{(0)} = \frac{e^{-\beta H^{(0)}}}{Z}. \tag{3.2}$$

where, $Z = \text{Tr}\left[e^{-\beta H^{(0)}}\right]$ is the partition function and $\beta = 1/k_B T$. The initial density matrix of our working fluid (target qubit) can be expressed by taking a partial trace

of 3-qubit system

$$\rho_{\mathcal{T}}^{(0)} = \mathrm{Tr}_{\mathcal{C},\mathcal{R}}\left[\rho_{\mathrm{th}}^{(0)}\right]. \tag{3.3}$$

3.3 Adiabatic Expansion:

Qubits are isolated from the heat bath and undergo finite-time adiabatic expansion. The adiabatic processes of the cycle are assumed to be generated by a time-dependent magnetic field [71, 73]. Here, $H^{(0)}$ at $t = 0$ is changed to $H^{(1)}$ at $t = \tau/2$ by driving the initial magnetic field as $B_z \to B_z/2$. The time evolution of the whole system is governed by the Liouville-von Neumann equation $\frac{d}{dt}\rho(t) = -[H(t), \rho(t)]$. The initial state as a condition $(t = 0)$ is $\rho(0) = \rho_{th}^{(0)}$, and $H(t)$ can be expressed as $H(t) = H^{(0)} + H_{\mathrm{drive}}$, where H_{drive} is given by

$$H_{\mathrm{drive}} = \hbar \sum_i (\omega_i - \omega_i') I_{iz} \sin(\pi t/\tau). \tag{3.4}$$

At the end of the expansion, the Hamiltonian of the whole system is

$$H^{(1)} = -\hbar \sum_i \omega_i' I_{iz} + \hbar \sum_{i \neq j} J_{ij} I_{iz} I_{jz}. \tag{3.5}$$

Here, $\omega_i' = \omega_i/2$ is the characteristic frequency at the end of the adiabatic stage. Considering the state of the 3-qubit system at the end of the expansion $(t = \tau/2$) as $\rho^{(1)} = \rho(\tau/2)$, we can find the state of the target qubit as $\rho_{\mathcal{T}}^{(1)} = \mathrm{Tr}_{\mathcal{C},\mathcal{R}}\left[\rho^{(1)}\right]$. Up to this point, we used the 3-qubit Hamiltonians in Eqs. (3.1, and 3.5). However, to find the work performed in the stage, we only need to deal with the target qubit. Therefore, we can write the local Hamiltonian for target qubit before the expansion as $H_{\mathcal{T}}^{(0)} = -\hbar\omega_{\mathcal{T}} I_z$ and at the end of the expansion as $H_{\mathcal{T}}^{(1)} = -\hbar\omega_{\mathcal{T}}' I_z$. Then, the work performed by the working fluid is

$$W_1 = \mathrm{Tr}\left[H_{\mathcal{T}}^{(0)} \rho_{\mathcal{T}}^{(0)}\right] - \mathrm{Tr}\left[H_{\mathcal{T}}^{(1)} \rho_{\mathcal{T}}^{(1)}\right]. \tag{3.6}$$

3.4 Heat Bath Algorithmic Cooling:

In this part of the engine, we usually need a cold heat bath to cool down our target qubit. Instead of using a cold heat bath, the working fluid treated in the same heat

bath as isochoric heating at temperature $T = 300$K. Reset, and compression qubits play their role in this stage. They help us to implement HBAC to cool down target qubit. In this stage Hamiltonian of the whole system given in Eq. (3.5). And the details of the cooling mechanism given in the Sec. 2.5. For each qubit, polarization is defined as the difference in the probability of up and down states, and easily found as

$$\epsilon_i = \tanh\left(\frac{\hbar\omega_i'}{2k_BT}\right). \tag{3.7}$$

In a closed quantum system, Shannon's bound limits the polarization of single spin in a collection of equilibrium spin system. Using partner pairing algorithm (PPA) let us increase the polarization of the target qubit. Consequently, the target qubit is cooled down beyond Shannon's bound [2]. After the first SWAP before PPA, polarizations of the target and reset qubits are equal to each other. The value of their polarization is given as zeroth iteration in Fig. 3.2 as $\sim 2.0\times10^{-5}$. Then, several rounds of PPA are applied. The target qubit reached a polarization above the Shannon limit as a result of the first iteration of PPA. The effective temperature of the target is determined by Eq. (3.8) and plotted in Fig. 3.3. Hence, target qubit cooled down to $\sim$ 50K. After seven iterations, the polarization of the target almost reached to its maximum value as $\sim 4.0\times10^{-5}$ and temperature of target cools down to $\sim$ 37K. At the end of PPA, the density matrix of the target qubit is given by Eq. (2.73) as

$$\rho_{\mathcal{T}}^{(2)} = \mathrm{Tr}_{\mathcal{C},\mathcal{R}}\left[\rho^{(1,5)}\right], \tag{3.8}$$

where the 1st index of the 3-qubit density matrix $\rho^{(1,5)}$ stands for the stage of the cycle and 2nd index from 0 to 5 indicates the state after each process of HBAC (see Sec. 2.5).

The applied algorithm in this stage is done by external radio frequency (rf) field in the heat bath at temperature $T = 300$ K. We consider these rf pulses as a cost of cooling. In Appendix A, we calculated the required energy for the cooling process. We can safely say that our cost is above the work output of the four-stroke engine which verifies the thermodynamical constraints.

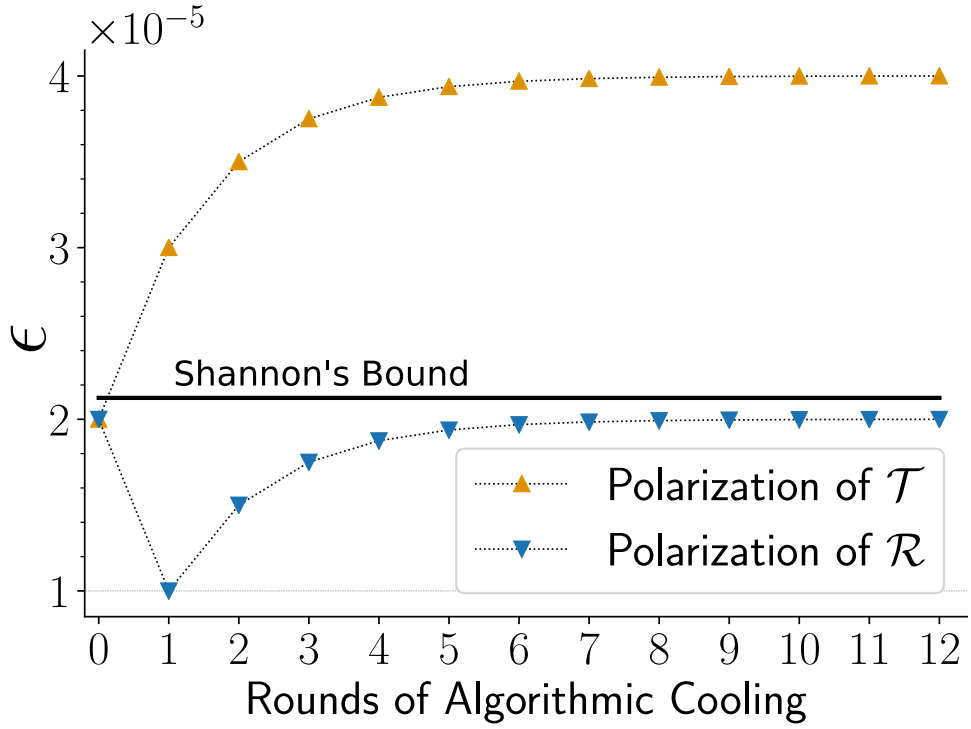

Figure 3.2: (Color online) The polarization ϵ (dimensionless) calculated by using the Eq. (3.8) for each round of algorithmic cooling. The target and reset qubits polarizations calculated by taking into account the perfectly applied quantum logic gates in terms of several rounds of the PPA. The black line shows Shannon's limit of polarization. The polarization of the target qubit has exceeded this limit after the first iteration, and the reset qubit stays under this limit.

3.5 Adiabatic Compression:

The Liouville-von Neumann equation gives the time evolution of the whole system during the adiabatic processes. In the compression step, $H^{(1)}$ at $t = 0$ is changed to $H^{(0)}$ at $t = \tau/2$ by driving back the magnetic field as $B_z/2 \rightarrow B_z$. The initial state $(t = 0)$ of the total system is $\rho(0) = \rho^{(1,5)}$ before adiabatic compression. The state of the whole system after adiabatic compression $(t = \tau/2)$ can be written as $\rho^{(3)} = \rho(\tau/2)$. Then, we can find the density matrix of the target qubit as $\rho_{\mathcal{T}}^{(3)} = \mathrm{Tr}_{\mathcal{C},\mathcal{R}}[\rho^{(3)}]$.

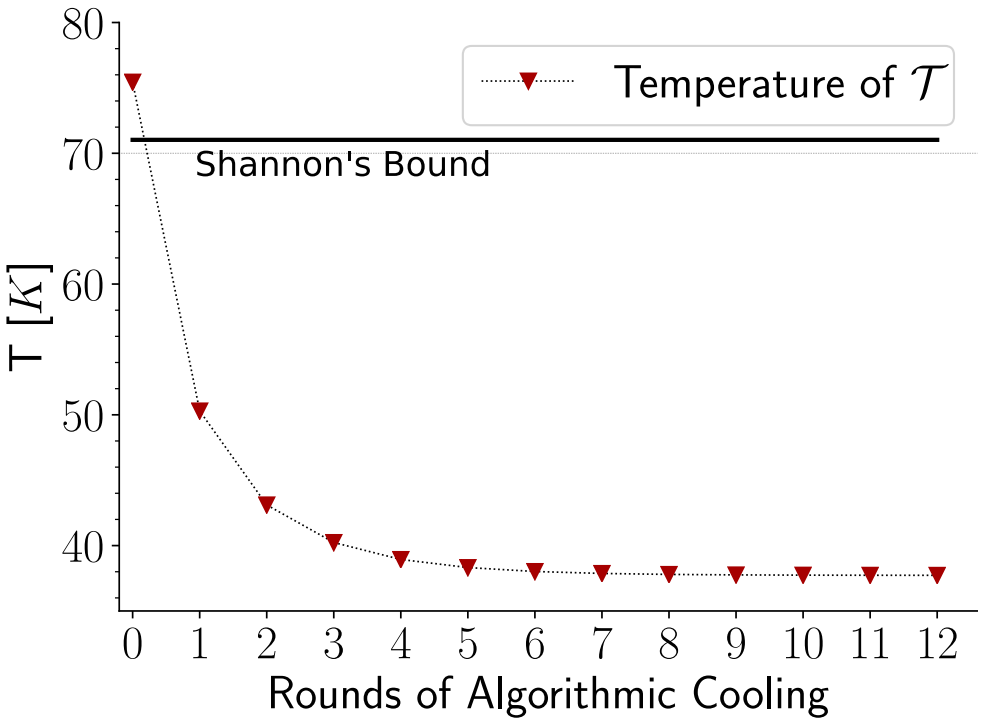

Figure 3.3: (Color online) The effective temperature of target qubit calculated by using the relation between temperature and polarization given in Eq. (3.8). The black line shows the corresponding Shannon's limit of temperature. The effective temperature of the target qubit has exceeded this limit after the first iteration.

The work performed by the target qubit in this process can be written as

$$W_2 = \mathrm{Tr}\left[H_{\mathcal{T}}^{(1)}\rho_{\mathcal{T}}^{(2)}\right] - \mathrm{Tr}\left[H_{\mathcal{T}}^{(0)}\rho_{\mathcal{T}}^{(3)}\right]. \tag{3.9}$$

After this compression, the four-stroke algorithmic engine cycle is complete for the target qubit with state $\rho_{\mathcal{T}}^{(3)}$. And, the states of the compression, and reset qubits are $\rho_{\mathcal{C}}^{(3)} = \mathrm{Tr}_{\mathcal{T},\mathcal{R}}[\rho^{(3)}]$ and $\rho_{\mathcal{R}}^{(3)} = \mathrm{Tr}_{\mathcal{T},\mathcal{C}}[\rho^{(3)}]$ respectively. The next cycle again starts with isochoric heating part and brings whole system to thermal state given in Eq.(3.2). This thermal state can be considered as injection state when we first started the cycle. After, the entire state of our system resets in every cycle with state $\rho^{(3)}$. Our choice of the order of the cycle steps is not unique and only for description purposes. As long as the cyclic order of the steps is respected, any of them can be designated

as a last step.

3.6 Work and Power Output:

The total work done by the working fluid at the end of adiabatic stages can be found as $W = W_1 + W_2$. Alternatively, the same entire work can also be calculated, from the isochoric stage and algorithmic cooling stage, using the relation; $W = Q_{\text{in}} - Q_{\text{out}}$ where, $Q_{\text{in}} = \text{Tr}\left[H_{\mathcal{T}}^{(0)}(\rho_{\mathcal{T}}^{(0)} - \rho_{\mathcal{T}}^{(3)})\right]$, and $Q_{\text{out}} = \text{Tr}\left[H_{\mathcal{T}}^{(1)}(\rho_{\mathcal{T}}^{(1)} - \rho_{\mathcal{T}}^{(2)})\right]$ are the heat absorbed ($Q_{\text{in}} > 0$) and released ($-Q_{\text{out}} < 0$) in these stages. In Fig. 3.4 , we plot the heat absorbed and released by the target qubit as per rounds of PPA. As the number of iterations increases, we observe that the absorbed heat increases more than the heat released. After the first iteration, the target qubit absorbed $\sim 5 \times 10^{-7}$J/mol of heat and released $\sim 2.5 \times 10^{-7}$J/mol of heat. As a result, $\sim 2.5 \times 10^{-7}$J/mol work was performed. In Fig. 3.4 , after seven iterations, the target qubit almost reaches the maximum value of the heat that it can absorb or release. Absorbed and released heat from qubit in the cycle at this iteration is $\sim 3.5 \times 10^{-7}$J/mol and $\sim 7.2 \times 10^{-7}$J/mol. Then, maximum work output of the cycle is $\sim 3.75 \times 10^{-7}$J/mol.

To see the difference in power output caused by the algorithmic cooling and isochoric cooling, we numerically simulated a standard quantum Otto cycle cooled by isochoric cooling. Here, we imagined cold baths corresponding to the temperatures in Fig. 3.3, and we take the same parameters as we used for a four-stroke algorithmic heat engine. In the isochoric heating stage, we used $\sim$ 300 K hot reservoir. In the adiabatic stages, we drive the frequency of target qubit ($\omega_{\mathcal{T}} \rightleftarrows \omega'_{\mathcal{T}}$). The states of the target qubit at the end of isochoric cooling are equivalent to states at the end of algorithmic cooling. By this way, the work output of this standard QOE cooled by isochoric stage will be same as the cycle cooled by HBAC. In Fig. 3.5; For a four-stroke algorithmic heat engine, the work produced by the target qubit rapidly increases with the number of iterations, it remains constant after a specific iteration of the PPA. The reason for this behavior is that the HBAC can cool down the target qubit up to a certain limit [4, 37, 42, 45]. While for a standard QOE, it increases due

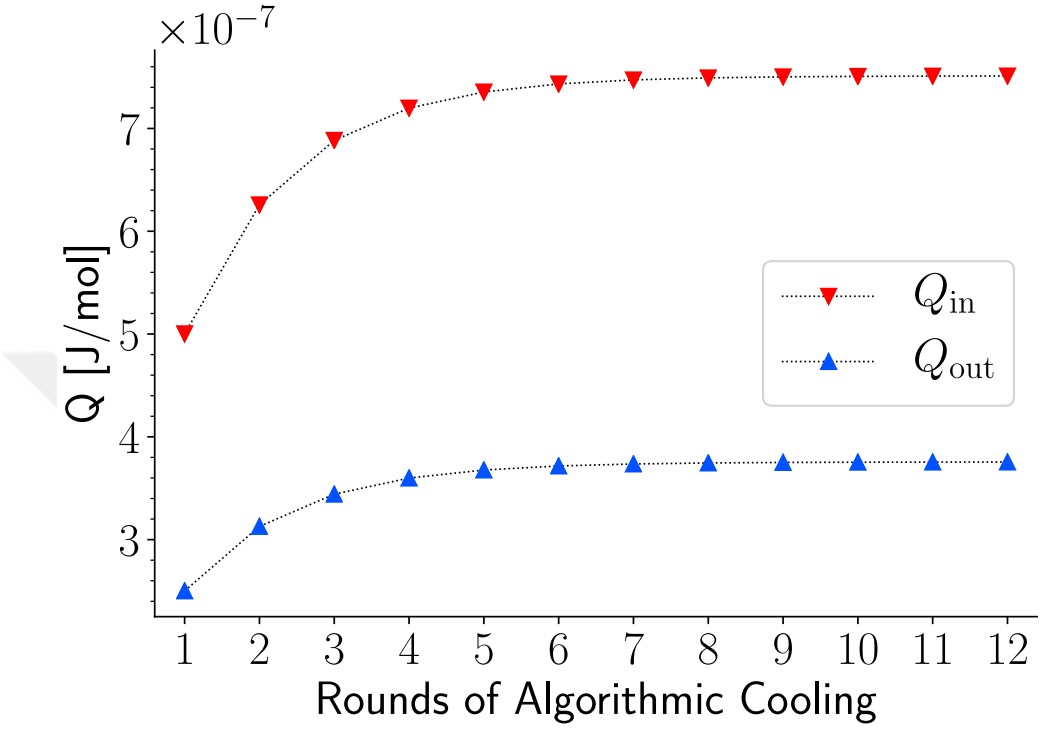

Figure 3.4: (Color online) Heat absorbed and released in a four-stroke cycle by the target qubit in the isochoric process (Q_{in}) and algorithmic cooling process (Q_{out}) for per rounds of PPA.

to the temperatures of the imagined cold baths. The amount of work corresponding to temperatures of ~ 50K is $\sim 2.5 \times 10^{-7}$J/mol and for ~ 37K it is $\sim 3.75 \times 10^{-7}$J/mol.

The adiabatic stages of the cycle are fast compared to the isochoric stages for a quantum Otto cycle using NMR system as its working fluid [35]. Hence, we can estimate the power output of cycles, only taking isochoric steps and HBAC. In isochoric stages, we need to wait for the thermalization of target qubit with the heat bath ($\tau_{\mathcal{T}}$). However, in algorithmic cooling stage, the relaxation time of reset qubit plays an important role. A single iteration of PPA requires two reset process. Denoting the number of iterations by n, we can write the total time requires to complete the algorithmic cooling stage as $\tau_{\mathcal{R}}(2n+1)$. Since both of the engines have the same work output, including the isochoric heating stage the power output of the

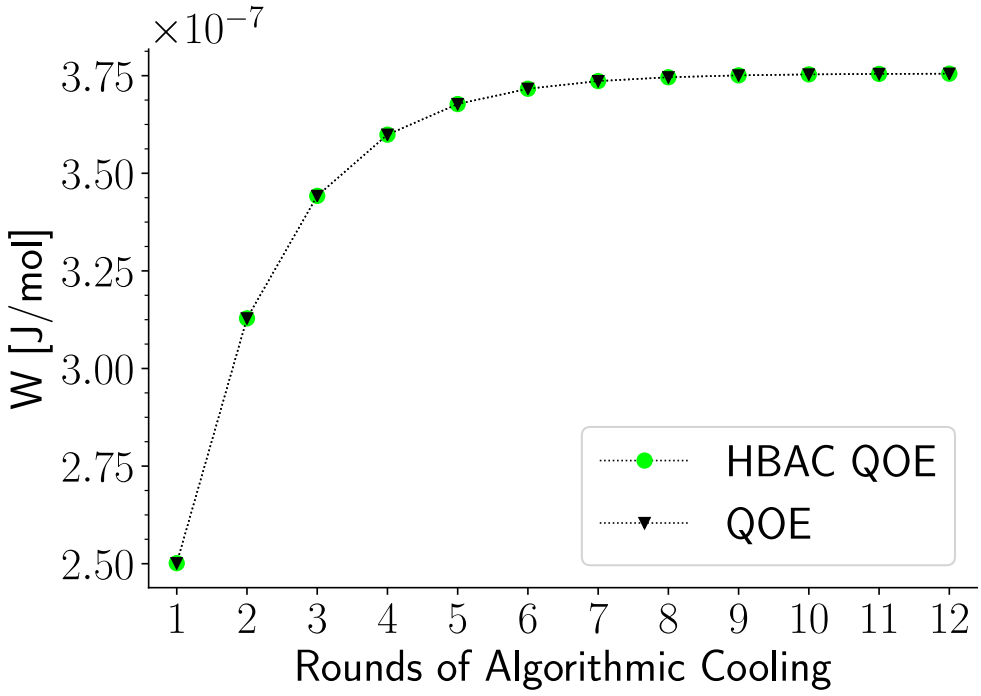

Figure 3.5: (Color online) Work obtained, in a four-stroke cycle per number of iteration of PPA, from target qubits of one mol of TCE cooled by HBAC. And work obtained from a mol of qubits, which are cooled by isochoric stage to temperatures corresponding in Fig 3.3.

algorithmic heat engine becomes

$$P = \frac{W}{(\tau_{\mathcal{T}} + \tau_{\mathcal{R}}(2n+1))}, \tag{3.10}$$

where, $\tau_{\mathcal{T}}$ and $\tau_{\mathcal{R}}$ are relaxation times of the Carbon1 and the Hydrogen qubits from the Table 3.1, respectively. In the case of standard quantum Otto cycle, the thermalization time in the cooling stage depends only on $\tau_{\mathcal{T}}$. Including the isochoric heating step, the power output becomes

$$P = \frac{W}{2\tau_{\mathcal{T}}}. \tag{3.11}$$

As long as $\tau_{\mathcal{R}}(2n+1)) < \tau_{\mathcal{T}}$ is satisfied, which is the case up to 5th iteration of PPA with our parameters, then algorithmic heat engines will give more output compared

to standard QOEs. In Fig. 3.6, we plot power outputs for both heat engines. We see that the second iteration of PPA gives maximum power output as $\sim 5.2 \times 10^{-9}$ Watt/mol for algorithmic heat engine. As we can see, the number of iteration of PPA

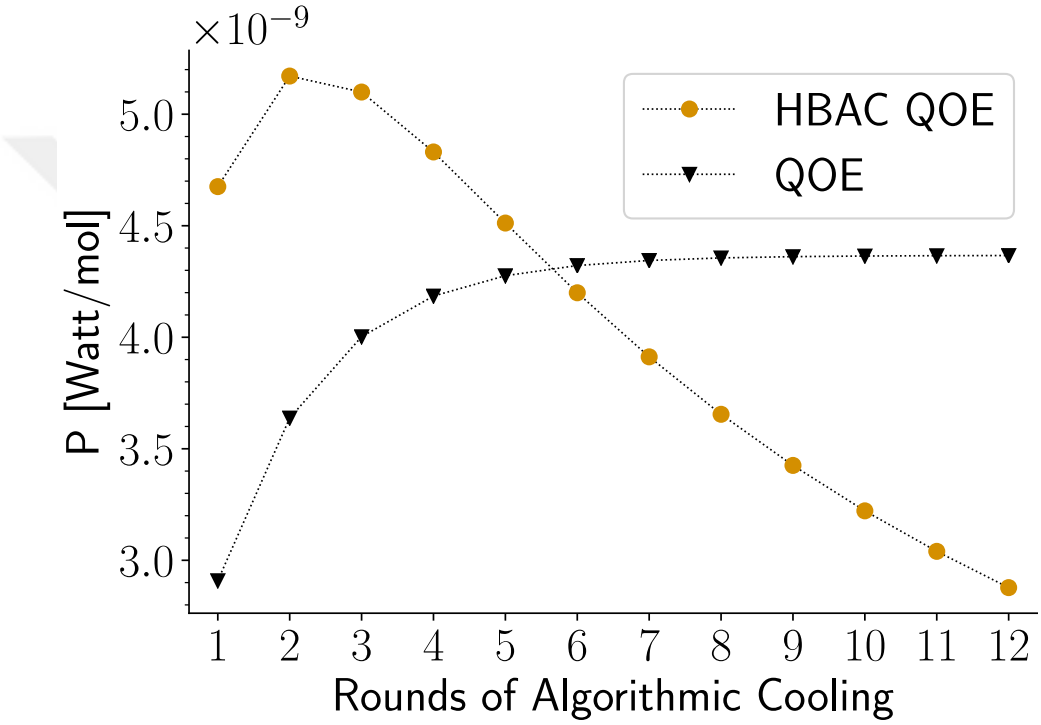

Figure 3.6: (Color online) Power output for a four-stroke cycle per number of iteration of PPA, from target qubit of one mol TCE, cooled by HBAC and from a mol of qubits cooled by isochoric stage to temperatures corresponding in Fig 3.3.

is critical due to the optimum operation of the algorithmic quantum heat engine. More repetition means more R operation for the cycle so that the time required to complete the engine increases. As expected, the power output of the four-stroke algorithmic heat engine decreases as the number of iteration increased. After the fifth iteration of PPA, the standard QOE using the isochoric cooling stage can dominate the engine using the algorithmic cooling stage. Accordingly, the optimum choice of the number of rounds for PPA is two for our four-stroke model system. Such a choice optimizes the power output of the cycle yielding high power performance.

It is vital to distinguish the cost paid to generate quantum gates from the cost to maintain the states of target qubit. The householding cost to maintain states in the working fluid can reduce thermodynamical efficiency [82, 83]. In our case, we do not need to maintain target qubit states after the gates we have applied during the HBAC stage. The cost of generation of quantum gates is not included to thermodynamical efficiency of engines. Thus, we do not include the cost of algorithmic cooling to the efficiency of the engines. The efficiency of the cycle is determined by $\eta = 1 - \omega'_{\mathcal{T}}/\omega_{\mathcal{T}}$ and for this engine $\eta = 0.5$. Further, to see how the coupling terms affect the engine work output, we take the interaction terms zero in the Hamiltonian and compare it with our results. Our numerical simulation shows the coupling between qubits brings a difference in the 9th order of magnitude to work output. Therefore we can ignore the effect of reset and compression qubits other than the algorithmic cooling step.

Chapter 4

TWO STROKE ALGORITHMIC QUANTUM HEAT ENGINE

By saying the two-stroke engine, we remark the original idea of the two-step work extraction is given in Ref. [5], and it is called there as alternative Otto cycle. The idea is based upon earlier ones, by Seth Lloyd on NMR implementation of a quantum Maxwell demon [84]. It allows for genuine, all-quantum algorithmic steps to harvest work in contrast to the approach of mimicking classical engine cycles in quantum systems. Alternative Otto cycle is indeed a full quantum alternative to Otto cycle, it replaces the cooling and adiabatic stages with HBAC and SWAP operations (or series of CNOT gate operations) and hence we compare it with the Otto cycles. Our approach is to come up with a quantum machine harvesting incoherent resources by cyclic quantum operations, analog of quantum computers harvesting coherent (information) resources. As the working substance for two-stroke QOEs, we again chose the target qubit of the 3-qubit system, but with an extra qubit coupled to the target qubit (see Fig. 4.1). In this engine, we have two qubits considered as working fluids.

4.1 The Working Fluid

We also investigate two-stroke QOE that is proposed in Refs. [5, 18]. To construct it, we need to take two qubits donated as $\mathcal{S}$ and $\mathcal{T}$ as the working fluid. First, two qubits are isolated from each other. One of the qubits contacts with a heat bath at temperature T until it reaches equilibrium. Our purpose is to cool the other qubit within the same heat bath utilizing algorithmic cooling. Hence we need another two qubits for this process as compression qubit and reset qubit. This part is considered as two isochoric processes for the heat engine. Second, two qubits decouple from

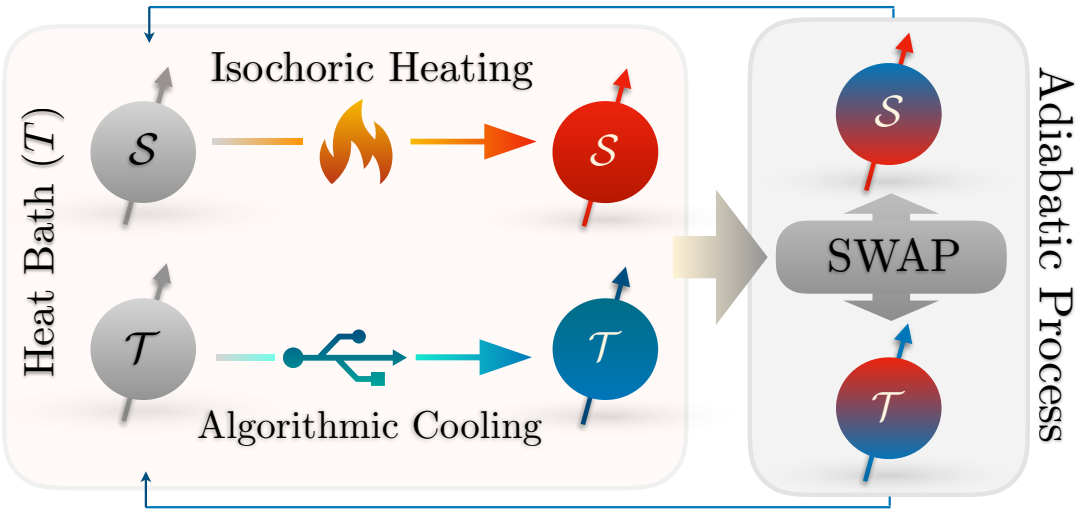

Figure 4.1: (Color online) Two-stroke algorithmic quantum heat engine operating in a single heat bath at temperature T. It has an isochoric heating process, and the algorithmic cooling process happens at the same time. Then, one adiabatic process using SWAP operation.

the heat bath. Then, the SWAP operation is performed between these two qubits (see Fig. 4.2). Local Hamiltonian of the qubit $\mathcal{S}$ and qubit $\mathcal{T}$ can be written as $H_{\mathcal{S}} = -\hbar\omega_{\mathcal{S}} I_z$ and $H_{\mathcal{T}} = -\hbar\omega_{\mathcal{T}} I_z$, respectively. Density matrix of qubit $\mathcal{S}$, at the end of the isochoric stage is a thermalized state given by $\rho_{\mathcal{S}}^{(1)} = e^{-\beta H_{\mathcal{S}}}/Z$. For the algorithmic cooling, again we take a system with Hamiltonian given in Eq. (3.1). Initially, assume that this three-qubit system is in a thermal equilibrium state ($\rho^{(1)}$) with the heat at temperature $T = 300$ K. Then we can cool down the qubit $\mathcal{T}$, using the algorithmic cooling given in the Sec. 2.5. The density matrix of qubit $\mathcal{T}$ at the end of HBAC can be written as $\rho_{\mathcal{T}}^{(1)} = \mathrm{Tr}_{\mathcal{C},\mathcal{R}}\left[\rho^{(1,5)}\right]$. It is assumed that the coupling between $\mathcal{S}$ and $\mathcal{T}$ qubits are small compared to $\omega_{\mathcal{S}}$ and $\omega_{\mathcal{T}}$. Thus, the density matrix of the total working fluid can be expressed as

$$\rho_{\mathcal{S},\mathcal{T}}^{(1)} \approx \rho_{\mathcal{S}}^{(1)} \otimes \rho_{\mathcal{T}}^{(1)}. \tag{4.1}$$

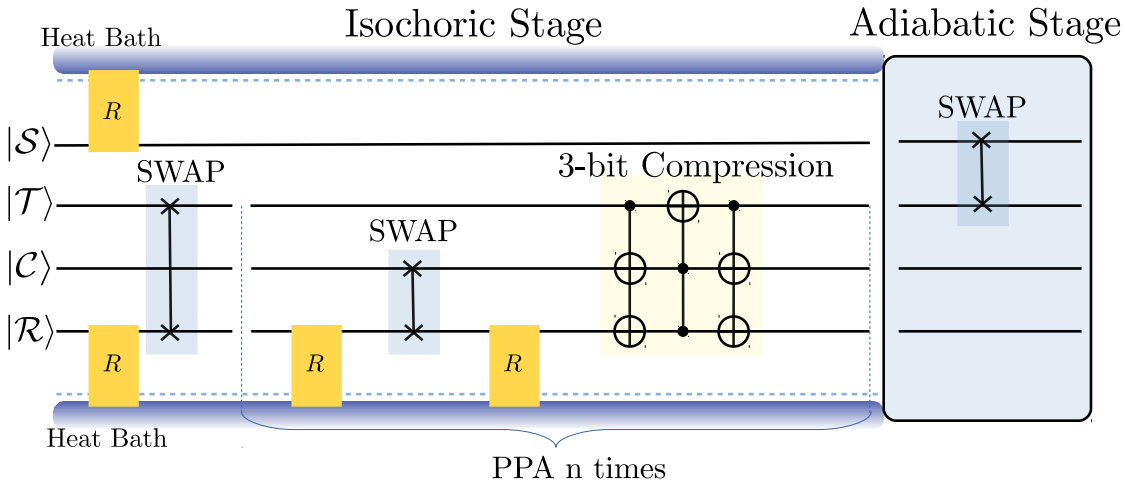

Figure 4.2: Quantum circuit demonstrating the two-stroke heat bath algorithmic cooled quantum Otto engine. $|\mathcal{S}\rangle$ stands for qubit $\mathcal{S}$ and $|\mathcal{T}\rangle$ for qubit $\mathcal{T}$. Here, isochoric heating demonstrated as R operation and applied only one time on qubit $\mathcal{S}$. For qubit $\mathcal{T}$, PPA applied, and it is given in Sec. 2.5. After these two processes finished the SWAP operation applied between two qubits and the cycle is completed with the adiabatic process.

In the adiabatic process, a SWAP gate is applied to exchange the states of $\mathcal{S}$ and $\mathcal{T}$ qubits

$$\rho^{(2)}_{\mathcal{S},\mathcal{T}} = \text{SWAP}\left(\rho^{(1)}_{\mathcal{S},\mathcal{T}}\right)\text{SWAP}^{\dagger}. \tag{4.2}$$

At the end of the cycle, density matrices of individual qubits become

$$\rho^{(2)}_{\mathcal{S}} = \text{Tr}_{\mathcal{T}}\left[\rho^{(2)}_{\mathcal{S},\mathcal{T}}\right], \quad \rho^{(2)}_{\mathcal{T}} = \text{Tr}_{\mathcal{S}}\left[\rho^{(2)}_{\mathcal{S},\mathcal{T}}\right]. \tag{4.3}$$

4.2 Work and Power Output

Heat absorbed by the qubit $\mathcal{S}$ calculated as follows

$$Q_{\text{in}} = \text{Tr}\left[H_{\mathcal{S}}(\rho^{(1)}_{\mathcal{S}} - \rho^{(2)}_{\mathcal{S}})\right], \tag{4.4}$$

and the heat released by the qubit $\mathcal{T}$ is

$$Q_{\text{out}} = \text{Tr}\left[H_{\mathcal{T}}(\rho_{\mathcal{T}}^{(2)} - \rho_{\mathcal{T}}^{(1)})\right]. \tag{4.5}$$

The net work is evaluated by $W = Q_{\text{in}} - Q_{\text{out}}$, with efficiency $\eta = 1 - \omega_{\mathcal{T}}/\omega_{\mathcal{S}}$. To get a positive work, the frequency of qubit $\mathcal{S}$ needs to be higher than the frequency of the qubit $\mathcal{T}$ ($\omega_{\mathcal{S}} > \omega_{\mathcal{T}}$). In addition, $T > T_{\mathcal{T}}(\omega_{\mathcal{S}}/\omega_{\mathcal{T}})$ needs to be satisfied. Here $T_{\mathcal{T}}$ is the temperature of target qubit in HBAC. Positive work conditions than can be expressed as

$$\omega_{\mathcal{T}} < \omega_{\mathcal{S}} < \omega_{\mathcal{T}}\frac{T}{T_{\mathcal{T}}}. \tag{4.6}$$

The work output of the two-stroke algorithmic quantum heat engine depends on the $\omega_{\mathcal{S}}$ and the number of iteration applied in the algorithmic cooling process. Fig. 4.3 shows the relation between the work output and $\omega_{\mathcal{S}}$, for different number of iterations. When the number of iterations of the PPA increases, the best work output also increases. However, after some iteration, it remains almost constant due to limiting of the PPA to cool the qubit $\mathcal{T}$. It is found that for 580 MHz, we almost get the best work output at 5th iteration as $\sim 3.0 \times 10^{-6}$ J/mol. But this frequency does not give us the best work output at 1st iteration. With 430 MHz frequency, we get $\sim 1.5 \times 10^{-6}$ J/mol maximum work output in the 1st iteration.

The adiabatic stage is evaluated by a SWAP operation, which is fast compared to the HBAC. Relaxation time of the $\mathcal{S}$ qubit may be estimated by considering spectral density functions $J(\omega, t_c)$, where t_c is the correlation time [49, 85]. If we look for the optimum power output, the $\omega_{\mathcal{S}}$ is close to the frequency of the $\mathcal{R}$ qubit. If the environmental effects are the same, t_c may be assumed to be the same for the $\mathcal{R}$ and $\mathcal{S}$ qubit. As a result, we can say that the $\mathcal{S}$ qubit is thermalized until the HBAC process is complete. Thus, estimation of the power output for a two-stroke algorithmic heat engine depends only on the algorithmic cooling stage. Then, we can write power output as

$$P = \frac{W}{\tau_{\mathcal{R}}(2n+1)} \tag{4.7}$$

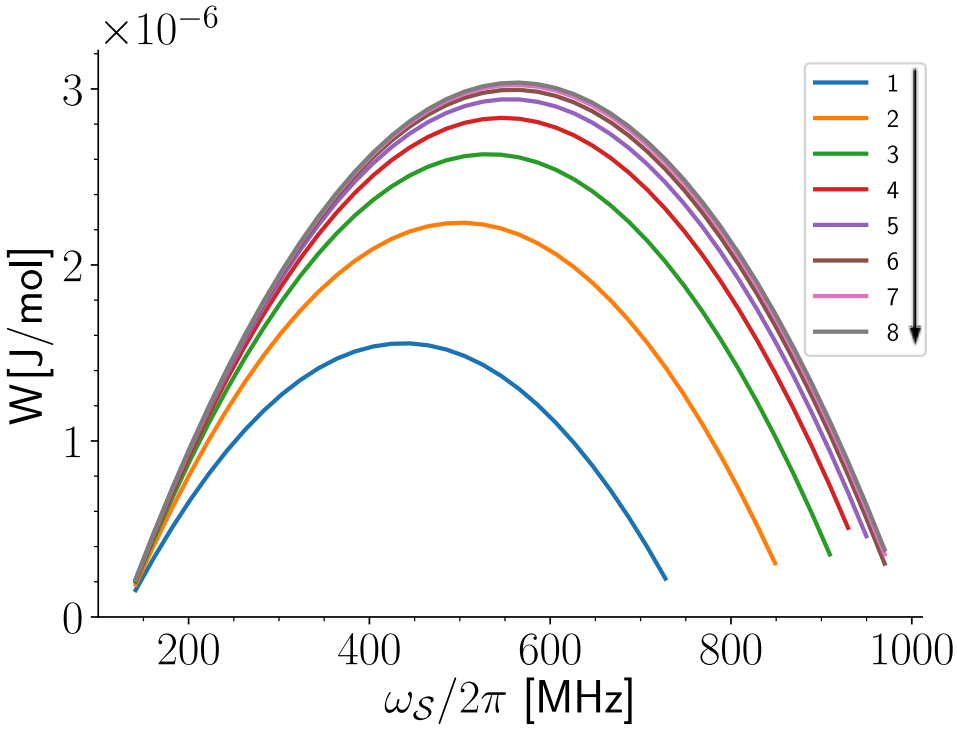

Figure 4.3: (Color online) Positive work obtained in two-strokes HBAC-QOE as a function of $\omega_{\mathcal{S}}$. The legend of the plot shows the number of rounds of PPA applied to qubit $\mathcal{T}$ and the direction of the arrow indicates an increase in work output from 1st iteration to 8th iteration.

considering the relaxation time of reset qubit and the number of iterations of PPA. The relaxation time of Hydrogen ($\tau_{\mathcal{R}}$) is given in Table 3.1. In Fig. 4.4, we plotted the power output based on the frequency of $\mathcal{S}$ qubit for different iteration numbers. As expected, the power of the two-stoke algorithmic machine decreases as the number of iterations increases in contrast to the work. The optimum value is given as $\sim 1.47 \times 10^{-7}$ Watt/mol during the 1st iteration with 430 MHz frequency of $\mathcal{S}$ qubit. If we compare these results to four-stroke quantum Otto cycles both cooled by HBAC and isochoric cooling, we see that the two-stroke cycle gives more work and power output. The efficiency of the cycle as a function of $\omega_{\mathcal{S}}$ is given above. Taking the optimum value for the power output during the 1st iteration with 430 MHz frequency

of qubit $\mathcal{S}$, we find the efficiency of the two-stroke machine as 0.7. In the HBAC at this iteration, our target qubit cooled the temperature of $\sim$ 27K and qubit $\mathcal{S}$ was in a heat bath at temperature $\sim$ 300K. If we look at the maximum efficiency at maximum power as $\eta_{me} = 1 - \sqrt{T_{\mathcal{T}}/T_{\mathcal{S}}}$ given by Curzon and Ahlborn [86], for these parameter it can be found as 0.7. Therefore, our results is also in the limit of this efficiency. Based on these results, we can say that the two-stroke algorithmic heat engine is more efficient than four-stroke cycles.

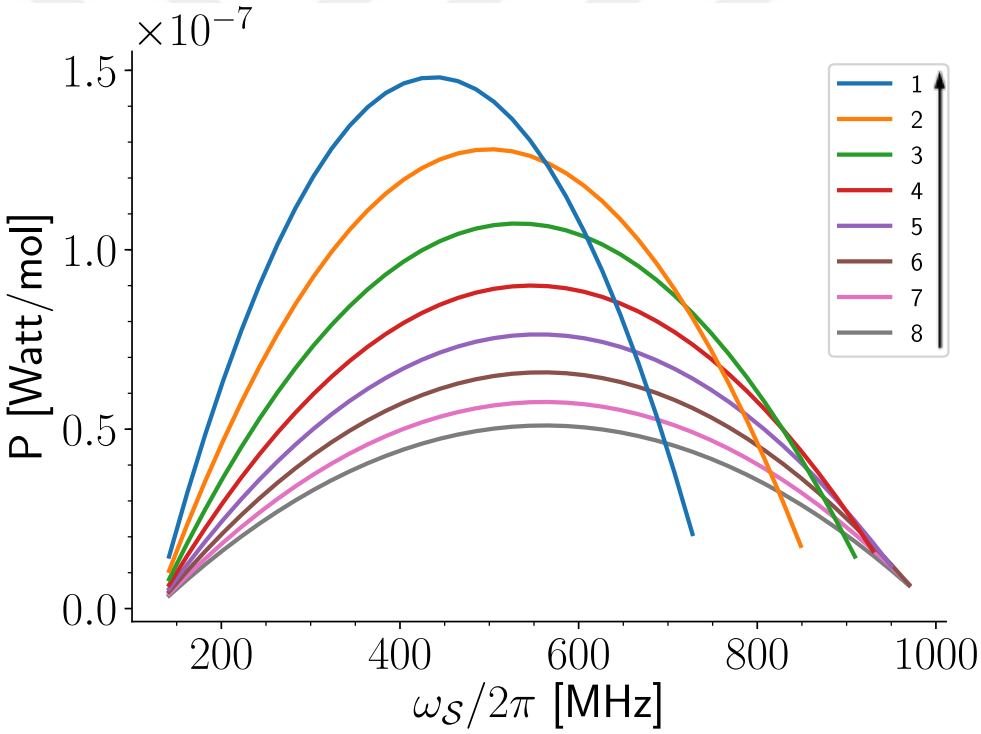

Figure 4.4: (Color online) Power output obtained in a two-stroke quantum Otto cycle for the different number of iterations of PPA as a function of $\omega_{\mathcal{S}}$. The legend of the plot shows the number of rounds of PPA applied to qubit $\mathcal{T}$ and the direction of the arrow indicates an increase in the power output from 8th iteration to 1st iteration.

To compare the algorithmic and the standard two-stroke heat engines, we again consider a two stroke machine cooled with isochoric cooling. For isochoric cooling, we imagined cold heat baths for temperatures corresponding to the algorithmic cooling

results for each iteration. When isochoric heating and adiabatic parts are applied in the same way, the work outputs that we get will be the same in these two machines. Assuming that the qubit $\mathcal{S}$ is thermalized faster than the qubit $\mathcal{T}$ during isochoric cooling, the power output of this standard two-stroke heat engine can only be determined by the thermalization time of the qubit $\mathcal{T}$ as $P = W/\tau_{\mathcal{T}}$. We can say; If $\tau_{\mathcal{R}}(2n+1)¡\ \tau_{\mathcal{T}}$ is satisfied, which is the case up to the 5th iterations of PPA with these parameters, our two-stroke algorithmic quantum heat engine gives more power output. Also, the second, lower temperature bath is challenging to implement in the context of NMR systems, and that's why our main objective is to be able to harvest work out of the single common environment using HBAC.

Chapter 5

CONCLUSIONS

We have investigated the possible quantum Otto engines implementing HBAC instead of isochoric cooling. Conventional NMR setups do not let to change strength (huge) magnetic field along the z direction. To solve this restriction, NMR setup can be modified to change the strong magnetic field via gradient coils such as Magnetic Resonance Imaging (MRI) system. Besides, the sample always in a single entropy sink in NMR systems. This is a critical challenge to design QOEs, which requires two heat bath to extract work from NMR qubits. Using HBAC allows us to cool the working fluid in a single heat bath. Here we specifically showed this cooling process could be implemented to four-stroke and two-stroke QOEs. The isochoric cooling process of the cycle takes too much time compared to the HBAC. Comparing our results with a single spin NMR heat engine, utilizing the HBAC to QOEs improves the power output of the cycles up to a particular iteration of PPA. By using SWAP operations in place of adiabatic stages and HBAC instead of isochoric cooling a completely algorithmic quantum heat engine, which can be more powerful and fast relative to those based upon traditional heat engine cycles, is proposed. Such engines offer programmable quantum heat engines as analogs of quantum computers but for efficient harvesting and processing incoherent resources rather than coherent information resources.

Appendix A

COST OF HEAT BATH ALGORITHMIC COOLING

The cost of cooling target qubit using the HBAC in the engine examined by the coherent operations (radio frequency field (rf) applied externally to the system). Cost of coherent operations treated as the free energy change of the system [87–89] or can be estimated from absorption power of rf field applied to generate quantum gates.

A.1 Coherent Operations:

From Sec. 2.5.1, we know the states before and after the SWAP and COMP operations. Since the entropy of the whole system is invariant under a unitary operation, the free energy change for the first SWAP will be

$$\Delta F = \mathrm{Tr}\left[H^{(1)}(\rho^{(1,1)} - \rho^{(1,0)})\right]. \tag{A.1}$$

In the iterative part of PPA, for the first SWAP it will be

$$\Delta F' = \mathrm{Tr}\left[H^{(1)}(\rho^{(1,3)} - \rho^{(1,2)})\right], \tag{A.2}$$

and for COMP operation

$$\Delta F'' = \mathrm{Tr}\left[H^{(1)}(\rho^{(1,5)} - \rho^{(1,4)})\right]. \tag{A.3}$$

The total free energy change due to unitary operations will be

$$\Delta F_{\mathrm{tot}} = \Delta F + \Delta F' + \Delta F'' \tag{A.4}$$

In Fig. A.1, we plot total free energy change due to rounds of algorithmic cooling. From the plot we can see that our cost for unitary operations is above the work we

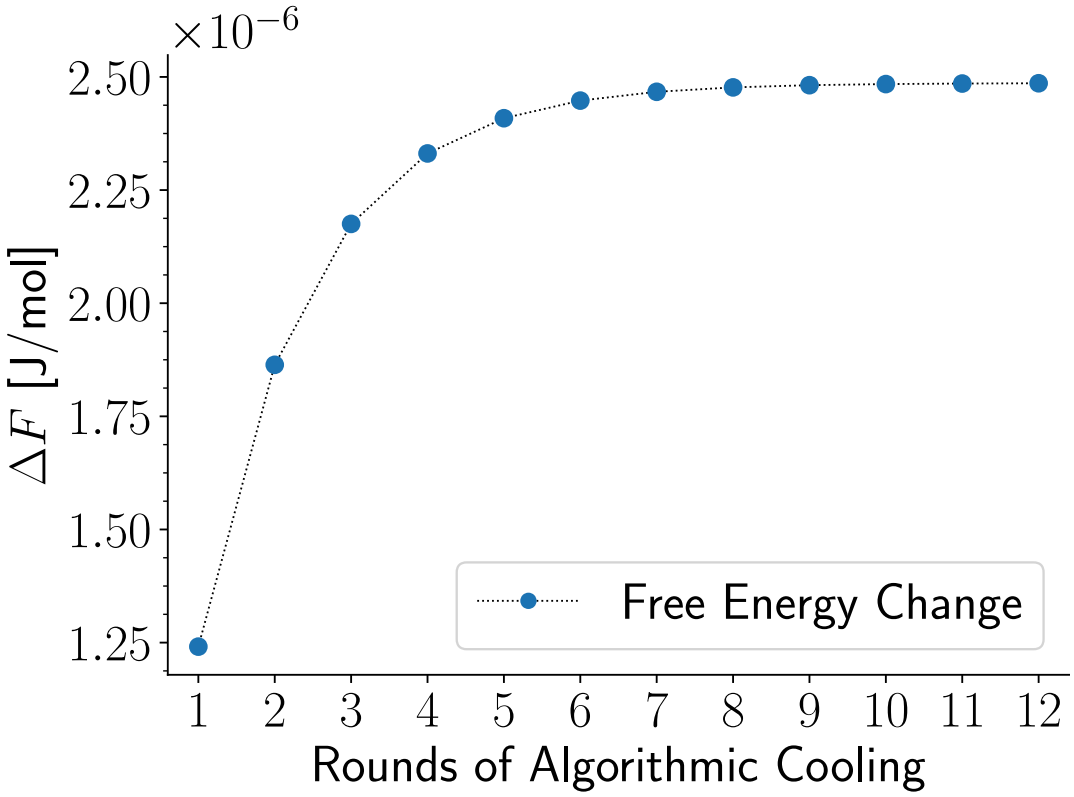

Figure A.1: (Color online) The total cost of cooling the target qubit by HBAC. It is obtained by the free energy change due to unitary operations.

gained from four stroke algorithmic heat engines, and for a single iteration, our cost is around $\Delta F \sim 1.2 \times 10^{-6}$ J/mol. After each unitary evolution in HBAC, the reset qubit is non-equilibrium with the heat bath. So, R operation is done by the bath, and heat released from the reset qubit to the thermal environment.

A.2 Rf Field Absorption Energy:

For a single pulse, we can calculate absorption energy, by a single qubit, using non-relativistic Fermi's Golden rule [49]. Unperturbed local Hamiltonian of the single qubit after adiabatic compression is $H_i^{(1)} = -\hbar\omega_i' I_z$. And the rf Hamiltonian as a

perturbation can be written as

$$H_{rf} = \frac{1}{2}\gamma_i \hbar B_{rf} \left(I_+ e^{-i\omega t} + I_- e^{i\omega t}\right) \tag{A.5}$$

For spin 1/2 system transition probability can be found as

$$W_{-\frac{1}{2}\to\frac{1}{2}} = \frac{\pi}{2}\gamma^2 B_{rf}^2 f(\omega) \tag{A.6}$$

where, $f(\omega)$ is related with shape of the pulse $\int f(\omega)d\omega = 1$. For instance, for the Lorentz shape it is described as $f(\omega) = \tau_2/\pi(1 + (\omega - \omega_i')^2\tau_2^2)$ Here, τ_2 is the transverse relaxation time. Usually, $\omega = \omega_i'$ and $f(\omega) = \tau_2/\pi$. If the difference in populations in a heat bath at temperature T can be written as $\sim \hbar\omega_i'/(2k_BT)$, then the amount of rf field energy absorbed per unit time by single qubit can be found as

$$\begin{aligned}\mathcal{P} &= \hbar\omega_i' \left(\frac{\hbar\omega_i'}{2k_BT}\right) W_{-\frac{1}{2}\to\frac{1}{2}} \\ &= \frac{\pi\hbar^2\omega_i'^2}{4k_BT}(\gamma_i^2 B_{rf}^2) f(\omega)\end{aligned}$$

Now we can determine pulse duration as $\theta_p = \gamma_i B_{rf} t_p$ and for $\pi/2$ pulse is can be found as $t_p = \pi/(2\gamma_i B_{rf})$. So total absorbed energy for single qubit will be

$$E_{abs} = \mathcal{P}t_p = \frac{\pi\hbar^2\omega_i'^2}{8k_BT}(\gamma_i B_{rf})\tau_2 \tag{A.7}$$

Radio frequency field is applied only one qubit during a CNot gate and the NMR pulse sequence of the CNot given as $R_x(\pi/2)U(1/2J)R_y(\pi/2)$, where $R_i(\theta_p)$ is the rotation matrix applied in i^{th} direction, and U is the unitary evolution due to the coupling of two qubits [47]. According to the first qubit orientation, the second qubit reversed or not reversed. For a single CNot, we need to apply two pulses in x and y direction. SWAP operation also can be decomposed into three CNot gate. So for a single SWAP, one needs six pulses, and for COMP gate we can assume it is around 10. In total, we approximately need 25 pulses for a single iteration of algorithmic cooling. At this stage, frequencies of target and compression qubit $\omega'_{\mathcal{T},\mathcal{C}} \approx 63$ MHz, and for reset qubit $\omega'_{\mathcal{R}} \approx 250$ MHz. The temperature of the bath is 300 K. To estimate a rough result for a typical Liquid State NMR system taking $\omega_i' \sim 100$ MHz, and

assuming $\gamma_i B_{rf} \sim 10^3$ Hz, and $\tau_2 \sim 10$ msec, we can find the total energy absorbed by single TCE molecule during cooling process as $E_{tot} \sim 2.6 \times 10^{-30}$ J. For 1 mol of TCE, it can be easily estimated as $E_{tot} \sim 1.6 \times 10^{-6}$ J/mol. This result is pretty close to above found by Eq.(A.4) for a single iteration.

A.3 Rf Field Energy:

We can also estimate the total energy given by every pulse due to the magnetic field. Since there will be losses to the environment, rf field energy that we applied will be higher than the free energy change or absorption energy by spins. The energy density of the applied magnetic field can be written as

$$u = \frac{1}{2\mu_0}|B_{rf}|^2 \tag{A.8}$$

Local pulse intensity is just multiplying this expression with c (speed of the field in vacuum).

$$I_p = cu = \frac{c}{2\mu_0}|B_{rf}|^2 \tag{A.9}$$

For a beam with a width of δ, the pulse energy can be written

$$U_p = I_p \pi(\delta/2)^2 t_p \tag{A.10}$$

Here, width δ is directly related with rf coil diameter and assuming it is $\delta \sim 1$ cm. Again pulse duration $t_p = \pi/(2\gamma B_{rf})$ sec, $\mu_0 = 4\pi \times 10^{-7}$ Tm/A give us $U_p \sim 9 \times 10^{-3}$ J.

As a result, we have $W < \Delta F < U_p$. Thus, our calculation of the cost of cooling the target qubit give us a result larger than the work output of the quantum Otto engines and verifies the thermodynamical constraints.

BIBLIOGRAPHY

[1] E. Köse, S. Çakmak, A. Gençten, I. K. Kominis, and Ö. E. Müstecaplıoğlu, "Algorithmic quantum heat engines," *Phys. Rev. E*, vol. 100, p. 012109, Jul 2019.

[2] Y. Atia, Y. Elias, T. Mor, and Y. Weinstein, "Algorithmic cooling in liquid-state nuclear magnetic resonance," *Phys. Rev. A*, vol. 93, p. 012325, Jan 2016.

[3] G. Brassard, Y. Elias, J. M. Fernandez, H. Gilboa, J. A. Jones, T. Mor, Y. Weinstein, and L. Xiao, "Experimental heat-bath cooling of spins," *The European Physical Journal Plus*, vol. 129, p. 266, Dec 2014.

[4] N. A. Rodríguez-Briones and R. Laflamme, "Achievable polarization for heat-bath algorithmic cooling," *Phys. Rev. Lett.*, vol. 116, p. 170501, Apr 2016.

[5] H. T. Quan, Y.-x. Liu, C. P. Sun, and F. Nori, "Quantum thermodynamic cycles and quantum heat engines," *Phys. Rev. E*, vol. 76, p. 031105, Sep 2007.

[6] X.-L. Huang, X.-Y. Niu, X.-M. Xiu, and X.-X. Yi, "Quantum stirling heat engine and refrigerator with single and coupled spin systems," *The European Physical Journal D*, vol. 68, p. 32, Feb 2014.

[7] G. Thomas and R. S. Johal, "Friction due to inhomogeneous driving of coupled spins in a quantum heat engine," *The European Physical Journal B*, vol. 87, p. 166, Jul 2014.

[8] T. Zhang, W.-T. Liu, P.-X. Chen, and C.-Z. Li, "Four-level entangled quantum heat engines," *Phys. Rev. A*, vol. 75, p. 062102, Jun 2007.

[9] X. L. Huang, H. Xu, X. Y. Niu, and Y. D. Fu, "A special entangled quantum heat

engine based on the two-qubit heisenberg xx model," *Physica Scripta*, vol. 88, no. 6, p. 065008, 2013.

[10] G. Thomas and R. S. Johal, "Coupled quantum otto cycle," *Phys. Rev. E*, vol. 83, p. 031135, Mar 2011.

[11] M. O. Scully, M. S. Zubairy, G. S. Agarwal, and H. Walther, "Extracting work from a single heat bath via vanishing quantum coherence," *Science*, vol. 299, no. 5608, pp. 862–864, 2003.

[12] G. F. Zhang, "Entangled quantum heat engines based on two two-spin systems with dzyaloshinski-moriya anisotropic antisymmetric interaction," *The European Physical Journal D*, vol. 49, p. 123, Jul 2008.

[13] S. Çakmak, F. Altintas, and Ö. E. Müstecaplıoğlu, "Lipkin-meshkov-glick model in a quantum otto cycle," *The European Physical Journal Plus*, vol. 131, p. 197, Jun 2016.

[14] K. Zhang, F. Bariani, and P. Meystre, "Quantum optomechanical heat engine," *Phys. Rev. Lett.*, vol. 112, p. 150602, Apr 2014.

[15] D. Türkpençe and O. E. Müstecaplıoğlu, "Quantum fuel with multilevel atomic coherence for ultrahigh specific work in a photonic carnot engine," *Phys. Rev. E*, vol. 93, p. 012145, Jan 2016.

[16] S. Chand and A. Biswas, "Single-ion quantum otto engine with always-on bath interaction," *EPL (Europhysics Letters)*, vol. 118, no. 6, p. 60003, 2017.

[17] S. Chand and A. Biswas, "Measurement-induced operation of two-ion quantum heat machines," *Phys. Rev. E*, vol. 95, p. 032111, Mar 2017.

[18] R. Uzdin, A. Levy, and R. Kosloff, "Equivalence of quantum heat machines, and quantum-thermodynamic signatures," *Phys. Rev. X*, vol. 5, p. 031044, Sep 2015.

[19] A. Alecce, F. Galve, N. L. Gullo, L. Dell'Anna, F. Plastina, and R. Zambrini, "Quantum Otto cycle with inner friction: Finite-time and disorder effects," *New J. Phys.*, vol. 17, no. 7, 2015.

[20] H. E. D. Scovil and E. O. Schulz-DuBois, "Three-level masers as heat engines," *Phys. Rev. Lett.*, vol. 2, pp. 262–263, Mar 1959.

[21] R. Alicki, "The quantum open system as a model of the heat engine," *Journal of Physics A: Mathematical and General*, vol. 12, no. 5, p. L103, 1979.

[22] N. Linden, S. Popescu, and P. Skrzypczyk, "How small can thermal machines be? the smallest possible refrigerator," *Phys. Rev. Lett.*, vol. 105, p. 130401, Sep 2010.

[23] R. Uzdin and R. Kosloff, "The multilevel four-stroke swap engine and its environment," *New Journal of Physics*, vol. 16, no. 9, p. 095003, 2014.

[24] D. Gelbwaser-Klimovsky, R. Alicki, and G. Kurizki, "Minimal universal quantum heat machine," *Phys. Rev. E*, vol. 87, p. 012140, Jan 2013.

[25] R. Kosloff and A. Levy, "Quantum heat engines and refrigerators: Continuous devices," *Annual Review of Physical Chemistry*, vol. 65, no. 1, pp. 365–393, 2014. PMID: 24689798.

[26] T. Feldmann and R. Kosloff, "Quantum four-stroke heat engine: Thermodynamic observables in a model with intrinsic friction," *Phys. Rev. E*, vol. 68, p. 016101, Jul 2003.

[27] J. Roßnagel, S. T. Dawkins, K. N. Tolazzi, O. Abah, E. Lutz, F. Schmidt-Kaler, and K. Singer, "A single-atom heat engine," *Science*, vol. 352, no. 6283, pp. 325–329, 2016.

[28] O. Abah, J. Roßnagel, G. Jacob, S. Deffner, F. Schmidt-Kaler, K. Singer, and E. Lutz, "Single-ion heat engine at maximum power," *Phys. Rev. Lett.*, vol. 109, p. 203006, Nov 2012.

[29] J. Klaers, S. Faelt, A. Imamoglu, and E. Togan, "Squeezed thermal reservoirs as a resource for a nanomechanical engine beyond the carnot limit," *Phys. Rev. X*, vol. 7, p. 031044, Sep 2017.

[30] J. Roßnagel, O. Abah, F. Schmidt-Kaler, K. Singer, and E. Lutz, "Nanoscale heat engine beyond the carnot limit," *Phys. Rev. Lett.*, vol. 112, p. 030602, Jan 2014.

[31] R. Dillenschneider and E. Lutz, "Energetics of quantum correlations," *EPL (Europhysics Letters)*, vol. 88, no. 5, p. 50003, 2009.

[32] C. B. Da, W. Niedenzu, Ö. E. Müstecapliolu, and G. Kurizki, "Multiatom quantum coherences in micromasers as fuel for thermal and nonthermal machines," *Entropy*, vol. 18, p. 244, jun 2016.

[33] J. P. S. Peterson, T. B. Batalhão, M. Herrera, A. M. Souza, R. S. Sarthour, I. S. Oliveira, and R. M. Serra, "Experimental characterization of a spin quantum heat engine," 2018.

[34] R. J. de Assis, T. M. de Mendonça, C. J. Villas-Boas, A. M. de Souza, R. S. Sarthour, I. S. Oliveira, and N. G. de Almeida, "Efficiency of a quantum otto heat engine operating under a reservoir at effective negative temperatures," *Phys. Rev. Lett.*, vol. 122, p. 240602, Jun 2019.

[35] S. Çakmak, F. Altintas, A. Gençten, and Ö. E. Müstecaplıoğlu, "Irreversible work and internal friction in a quantum otto cycle of a single arbitrary spin," *The European Physical Journal D*, vol. 71, p. 75, Mar 2017.

[36] D. K. Park, N. A. Rodriguez-Briones, G. Feng, R. Rahimi, J. Baugh, and R. Laflamme, *Heat Bath Algorithmic Cooling with Spins: Review and Prospects*, pp. 227–255. New York, NY: Springer New York, 2016.

[37] G. Brassard, Y. Elias, T. Mor, and Y. Weinstein, "Prospects and limitations of

algorithmic cooling," *The European Physical Journal Plus*, vol. 129, p. 258, Nov 2014.

[38] J. M. Fernandez, S. Lloyd, T. Mor, and V. Roychowdhury, "Algorithmic Cooling of Spins: A Practicable Method for Increasing Polarization," *Int. J. Quantum Inf.*, vol. 02, pp. 461–477, dec 2004.

[39] Y. Elias, J. M. Fernandez, T. Mor, and Y. Weinstein, "Optimal algorithmic cooling of spins," in *Unconventional Computation* (S. G. Akl, C. S. Calude, M. J. Dinneen, G. Rozenberg, and H. T. Wareham, eds.), pp. 2–26, Berlin, Heidelberg: Springer Berlin Heidelberg, 2007.

[40] P. O. Boykin, T. Mor, V. Roychowdhury, F. Vatan, and R. Vrijen, "Algorithmic cooling and scalable nmr quantum computers," *Proceedings of the National Academy of Sciences*, vol. 99, no. 6, pp. 3388–3393, 2002.

[41] D. Kafri and J. M. Taylor, "Algorithmic Cooling of a Quantum Simulator," jul 2012.

[42] S. Raeisi and M. Mosca, "Asymptotic bound for heat-bath algorithmic cooling," *Phys. Rev. Lett.*, vol. 114, p. 100404, Mar 2015.

[43] N. A. Rodríguez-Briones, J. Li, X. Peng, T. Mor, Y. Weinstein, and R. Laflamme, "Heat-bath algorithmic cooling with correlated qubit-environment interactions," *New Journal of Physics*, vol. 19, p. 113047, nov 2017.

[44] C. A. Ryan, O. Moussa, J. Baugh, and R. Laflamme, "Spin based heat engine: Demonstration of multiple rounds of algorithmic cooling," *Phys. Rev. Lett.*, vol. 100, p. 140501, Apr 2008.

[45] L. J. Schulman, T. Mor, and Y. Weinstein, "Physical limits of heat-bath algorithmic cooling," *Phys. Rev. Lett.*, vol. 94, p. 120501, Apr 2005.

[46] Y. Elias, J. M. Fernandez, T. Mor, and Y. Weinstein, "Optimal Algorithmic Cooling of Spins," *Isr. J. Chem.*, vol. 46, pp. 371–391, dec 2006.

[47] I. S. Oliveira, T. J. Bonagamba, R. S. Sarthour, J. C. Freitas, and E. R. deAzevedo, "4 - introduction to nmr quantum computing," in *NMR Quantum Information Processing*, pp. 137 – 181, Amsterdam: Elsevier Science B.V., 2007.

[48] M. Devoret, B. Huard, R. Schoelkopf, and L. Cugliandolo, *Quantum Machines: Measurement and Control of Engineered Quantum Systems*. Oxford University Press, 2011.

[49] A. Abragam, "Principles of nuclear magnetism," *Am. J. Phys.*, 1963.

[50] J. Goold, M. Huber, A. Riera, L. del Rio, and P. Skrzypczyk, "The role of quantum information in thermodynamicsa topical review," *Journal of Physics A: Mathematical and Theoretical*, vol. 49, no. 14, p. 143001, 2016.

[51] T. B. Batalhão, A. M. Souza, L. Mazzola, R. Auccaise, R. S. Sarthour, I. S. Oliveira, J. Goold, G. De Chiara, M. Paternostro, and R. M. Serra, "Experimental reconstruction of work distribution and study of fluctuation relations in a closed quantum system," *Phys. Rev. Lett.*, vol. 113, p. 140601, Oct 2014.

[52] R. Shankar, *Principles of Quantum Mechanics*. 1994.

[53] J. J. Sakurai and J. Napolitano, *Modern Quantum Mechanics*. Cambridge University Press, 2 ed., 2017.

[54] W. H. Louisell, *Quantum Statistical Properties of Radiation*. July 1990.

[55] W. C. Schieve and L. P. L. P. Horwitz, *Quantum statistical mechanics*. Cambridge University Press, 2009.

[56] K. Blum, *Density Matrix Theory and Applications*, vol. 64 of *Springer Series on Atomic, Optical, and Plasma Physics*. Berlin, Heidelberg: Springer Berlin Heidelberg, 2012.

[57] M. Kardar, *Statistical Physics of Particles*. 2012.

[58] R. R. Puri, *Mathematical Methods of Quantum Optics*. 2001.

[59] H. P. Breuer and F. Petruccione, *The Theory of Open Quantum Systems*. 2007.

[60] R. R. Alicki and K. K. Lendi, *Quantum dynamical semigroups and applications*. Springer-Verlag, 2007.

[61] A. Rivas and S. F. Huelga, *Open quantum systems : an introduction*. Springer, 2012.

[62] R. Alicki, "Invitation to quantum dynamical semigroups," may 2002.

[63] V. Gorini, A. Kossakowski, and E. C. G. Sudarshan, "Completely positive dynamical semigroups of nlevel systems," *Journal of Mathematical Physics*, vol. 17, no. 5, pp. 821–825, 1976.

[64] G. Lindblad, "On the generators of quantum dynamical semigroups," *Commun. Math. Phys.*, 1976.

[65] N. Bloembergen, E. M. Purcell, and R. V. Pound, "Relaxation effects in nuclear magnetic resonance absorption," *Phys. Rev.*, vol. 73, pp. 679–712, Apr 1948.

[66] A. REDFIELD, "The theory of relaxation processes.," in *Advances in Magnetic Resonance* (J. S. Waugh, ed.), vol. 1, Academic Press, 1965.

[67] I. Solomon, "Relaxation processes in a system of two spins," *Phys. Rev.*, vol. 99, pp. 559–565, Jul 1955.

[68] E. M. Purcell, "Spontaneous emission probabilities at radio frequencies," vol. 69, pp. 681+, 1946.

[69] M. Goldman, "Formal theory of spinlattice relaxation," *Journal of Magnetic Resonance*, vol. 149, no. 2, pp. 160 – 187, 2001.

[70] J. Gemmer, M. M. Michel, and G. Mahler, *Quantum thermodynamics : emergence of thermodynamic behavior within composite quantum systems*. Springer, 2004.

[71] S. Vinjanampathy and J. Anders, "Quantum thermodynamics," *Contemporary Physics*, vol. 57, no. 4, pp. 545–579, 2016.

[72] J. Millen and A. Xuereb, "Perspective on quantum thermodynamics," *New Journal of Physics*, vol. 18, p. 011002, jan 2016.

[73] R. Kosloff, "Quantum thermodynamics: A dynamical viewpoint," *Entropy*, vol. 15, no. 6, pp. 2100–2128, 2013.

[74] R. Alicki and R. Kosloff, *Introduction to Quantum Thermodynamics: History and Prospects*, pp. 1–33. Cham: Springer International Publishing, 2018.

[75] H. Spohn and J. L. Lebowitz, *Irreversible Thermodynamics for Quantum Systems Weakly Coupled to Thermal Reservoirs*, pp. 109–142. John Wiley Sons, Ltd, 2007.

[76] M. M. Wilde, *Quantum Information Theory*. Cambridge University Press, 2013.

[77] M. a. Nielsen and I. L. Chuang, *Quantum Computation and Quantum Information: 10th Anniversary Edition*. 2011.

[78] S. Y. Hou, Y. B. Sheng, G. R. Feng, and G. L. Long, "Experimental optimal single qubit purification in an NMR quantum information processor," *Sci. Rep.*, vol. 4, 2014.

[79] Z. Li, M. H. Yung, H. Chen, D. Lu, J. D. Whitfield, X. Peng, A. Aspuru-Guzik, and J. Du, "Solving quantum ground-state problems with nuclear magnetic resonance," *Sci. Rep.*, vol. 1, jun 2011.

[80] M. K. Henry, J. Emerson, R. Martinez, and D. G. Cory, "Localization in the quantum sawtooth map emulated on a quantum-information processor," *Phys. Rev. A*, vol. 74, p. 062317, Dec 2006.

[81] H. K. Cummins, C. Jones, A. Furze, N. F. Soffe, M. Mosca, J. M. Peach, and J. A. Jones, "Approximate quantum cloning with nuclear magnetic resonance," *Phys. Rev. Lett.*, vol. 88, p. 187901, Apr 2002.

[82] B. Gardas and S. Deffner, "Thermodynamic universality of quantum carnot engines," *Phys. Rev. E*, vol. 92, p. 042126, Oct 2015.

[83] A. Ü . Hardal and Ö. E. Müstecaplıoğlu, "Superradiant Quantum Heat Engine," *Sci. Rep.*, vol. 5, 2015.

[84] S. Lloyd, "Quantum-mechanical maxwell's demon," *Phys. Rev. A*, vol. 56, pp. 3374–3382, Nov 1997.

[85] A. G. Redfield, "On the theory of relaxation processes," *IBM Journal of Research and Development*, vol. 1, pp. 19–31, Jan 1957.

[86] F. L. Curzon and B. Ahlborn, "Efficiency of a carnot engine at maximum power output," *American Journal of Physics*, vol. 43, no. 1, pp. 22–24, 1975.

[87] F. Clivaz, R. Silva, G. Haack, J. B. Brask, N. Brunner, and M. Huber, "Unifying paradigms of quantum refrigeration: A universal and attainable bound on cooling,"

[88] F. Clivaz, R. Silva, G. Haack, J. B. Brask, N. Brunner, and M. Huber, "Unifying paradigms of quantum refrigeration: fundamental limits of cooling and associated work costs," 2019.

[89] M. Esposito and C. V. den Broeck, "Second law and landauer principle far from equilibrium," *EPL (Europhysics Letters)*, vol. 95, p. 40004, aug 2011.